Gondwana Research 26 (2014) 386–401

Contents lists available at ScienceDirect

Gondwana Research

journal homepage: www.elsevier.com/locate/gr

Timing and sources of pre-collisional Neoproterozoic sedimentation along the SW margin of the Congo Craton (Kaoko Belt, NW Namibia)

Jiří Konopásek [a,b,*], Jan Košler [a,b], Jiří Sláma [a,c], Vojtěch Janoušek [b]

[a] Department of Earth Science and Centre for Geobiology, University of Bergen, Allégaten 41, N-5007 Bergen, Norway
[b] Czech Geological Survey, Klárov 3, 118 21 Praha 1, Czech Republic
[c] Institute of Geology AS CR, v.v.i., Rozvojová 269, 165 00 Praha 6, Czech Republic

ARTICLE INFO

Article history:
Received 26 February 2013
Received in revised form 27 June 2013
Accepted 30 June 2013
Available online 19 July 2013

Handling Editor: T. Kusky

Keywords:
Detrital zircons
Protolith ages
Geochronology
Neoproterozoic Kaoko Belt
Namibia

ABSTRACT

Isotopic dating of detrital zircon populations from metasediments and of magmatic zircon from intercalated metavolcanic layers in the medium- to high-grade part of the Kaoko Belt in Namibia provides first robust constraints on the age of Neoproterozoic sedimentation along the southwestern margin of the Congo Craton. Dating of detrital zircons from metasediments directly overlying the cratonic basement shows maximum sedimentary ages of c. 1.00 and c. 1.45 Ga, and age populations comparable with known protolith ages from the gneisses of the Congo/Kalahari cratons. Dating of zircon from associated metavolcanics constrains the age of the earliest preserved sediments at c. 740–710 Ma.

Detrital zircon populations from the samples collected from the upper parts of the metasedimentary succession contain only small proportion of grains with ages similar to those from the Congo Craton. These samples show dominance of c. 1.00 Ga, c. 750 Ma and c. 650 Ma old zircon grains that are probably derived from the Punta del Este – Coastal Terrane (Dom Feliciano and Kaoko belts) that acted as an arc/back-arc domain at c. 650–630 Ma. Neodymium model ages for the samples of metasedimentary cover of the cratonic basement provide another evidence that the youngest preserved sediments could not have been derived from the Congo Craton.

Recognition of the Punta del Este – Coastal Terrane crust as a source region for the youngest pre-collisional sediments of the Kaoko Belt suggests that this terrane must have been in close proximity to the Congo Craton passive margin already some time prior to their mutual collision at c. 570–550 Ma. This is in accord with an interpretation that the c. 650–630 Ma arc/back-arc Punta del Este – Coastal Terrane has developed directly on top of, or very close to, the attenuated Congo Craton passive margin.

1. Introduction

The Neoproterozoic breakup of the Rodinia supercontinent and the formation of passive margins of the Congo and Kalahari cratons, which are now incorporated into orogenic belts of southwestern Africa (Fig. 1), started at c. 800–750 Ma by the deposition of rifting-related fluvial clastics that overlie the cratonic basement (Martin, 1965; Hedberg, 1979; Miller, 1983). The constraint for the timing of rifting along the southern Congo Craton margin comes from dating of granitoids and rhyolite lava flows at 756 and 746 Ma, respectively, that intrude and overlie the basal (Nosib Group) strata deposited along the southern slope of the cratonic basement of the Damara Belt (Hoffman et al., 1996; Fig. 1), and from dating of volcanic activity in the lower part of the sedimentary succession overlying the Nosib clastics in the Otavi Platform (760 Ma; Halverson et al., 2005; Fig. 1). Similar age of a rifting-related volcanic activity has been reported from the western margin of the Kalahari Craton by Frimmel et al. (1996, 2001) and Borg et al. (2003). The sedimentary succession overlying the Nosib clastics along the southern flank of the Congo Craton is represented by shallow-marine carbonate platform and upper-slope sediments of the Otavi Group in the Otavi Platform, and by the Swakop Group deeper-water, lower slope and basinal sediments in the Outjo and Swakop zones of the Damara Belt (Hoffmann and Prave, 1996; Prave, 1996; Hoffmann et al., 2004; Fig. 1). In the Swakop Zone, dating of an ash bed inside glacio-marine sediments situated approximately in the middle of the Swakop Group stratigraphic interval provided an age of 636 Ma (Hoffmann et al., 2004).

Sedimentary succession similar to that developed in the Otavi Platform is also present along the western flank of the Congo Craton in the eastern part of the Kaoko Belt (Hoffmann and Prave, 1996; Prave, 1996; Fig. 1). However, no datable intrusive rocks or syn-sedimentary volcanics have so far been reported from this region and the age of sedimentation for particular members of the sedimentary succession in this part of the Neoproterozoic sedimentary cover of the Congo Craton remains largely unconstrained. Towards the west, the Congo Craton gneissic basement crops out in tectonic windows and thrust sheets of the low- to high-

* Corresponding author at: Department of Earth Science and Centre for Geobiology, University of Bergen, Allégaten 41, N-5007 Bergen, Norway. Tel.: +47 55584719.
E-mail address: jiri.konopasek@geo.uib.no (J. Konopásek).

1342-937X/$ – see front matter © 2013 International Association for Gondwana Research. Published by Elsevier B.V. All rights reserved.
http://dx.doi.org/10.1016/j.gr.2013.06.021

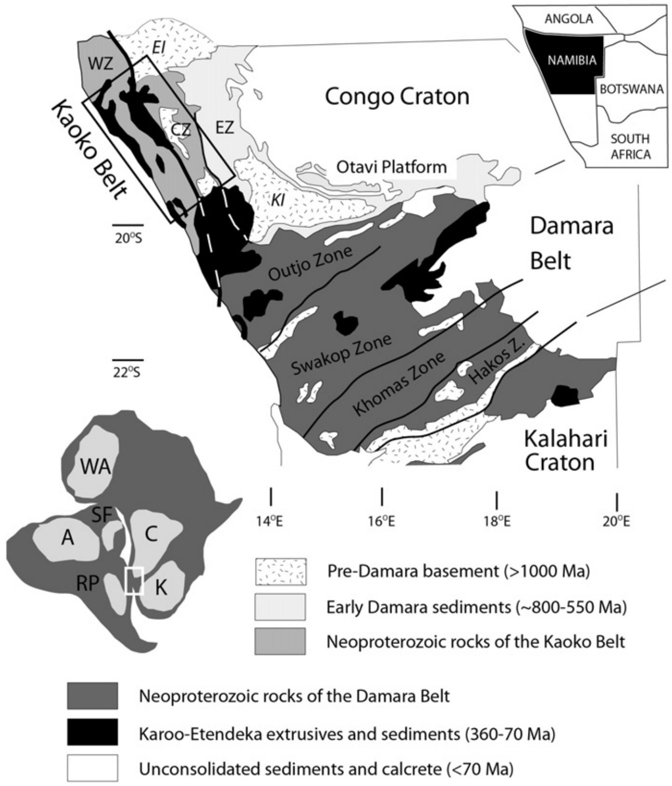

Fig. 1. Schematic tectonic map of the northern part of Namibia showing the position of the Kaoko and Damara belts. Tectonic units of the Kaoko Belt (WZ: Western Kaoko Zone; CZ: Central Kaoko Zone; EZ: Eastern Kaoko Zone; *KI*: Kamanjab Inlier; *EI*: Epupa Inlier) are after Miller (1983) and of the Damara Belt after Hoffmann et al. (2004). Cratons labeled in the inset are: A — Amazon; C — Congo; K — Kalahari; RP — Rio de la Plata; SF — São Francisco; and WA — West African. The Dom Feliciano Belt is located east of the Rio de la Plata Craton and the Gariep Belt is west of the Kalahari Craton. The black rectangle shows the location of Fig. 2.

grade Central and Western Kaoko zones (Figs. 1 and 2; Miller, 1983) and associated metasedimentary rocks may represent slope and basinal facies of its former Neoproterozoic sedimentary cover (Dingeldey et al., 1994; Goscombe, 1998a,b; Seth et al., 1998; Goscombe et al., 2003a; Kröner et al., 2004). Depositional age of metamorphosed sedimentary rocks in the Central and Western Kaoko zones is not known. While the metasedimentary succession in the easternmost part of the Central Kaoko Zone can be correlated with the sediments of the Outjo and Swakop zones (Guj, 1970; Dingeldey et al., 1994), the protolith age and the extent of metasedimentary rocks in more westerly parts of the Kaoko Belt are not entirely clear due to medium- to high-grade metamorphism and intense deformation. Moreover, the westernmost high-grade part of the Kaoko Belt is represented by the Coastal Terrane (Fig. 2), a unit interpreted as an arc/back-arc-type crustal block with the pre-collisional evolution independent of that recognized along the western flank of the Congo Craton (Goscombe et al., 2005; Goscombe and Gray, 2007). Very little is known about the metasedimentary rocks of the Coastal Terrane and the only indication of their sedimentary age comes from dating of interlayered bimodal metaigneous rocks that have been interpreted as metamorphosed syn-sedimentary volcanics and their protolith dated at c. 800 Ma (Konopásek et al., 2008). The measure of pre-collisional separation of the Coastal Terrane from the Congo Craton passive margin remains unclear, but the lack of relics of oceanic crust along the contact of the Kaoko Belt proper with the Coastal Terrain suggests that the latter may have never been separated from the passive margin of the Congo Craton by an oceanic domain (Goscombe and Gray, 2007).

In this study we present geochronological data from intermediate to felsic rocks that occasionally occur within prominent layers of metamorphosed mafic volcanics accompanying metasedimentary units that overlie the cratonic basement of the Kaoko belt proper. We also report zircon age spectra from surrounding metasediments, as well as from metasediments of the high-grade Coastal Terrane. Dating of the metamorphosed volcanic rocks and zircon provenance analysis, together with whole-rock Nd isotopic data, provide for the first time reliable information on the sedimentation age and source of the detritus in the medium- and high-grade parts of the Kaoko Belt, and constrain the role of the Coastal Terrane in its tectonic evolution.

2. Geology of the Kaoko Belt and previous opinion on timing of sedimentation

Miller (1983) divided the Kaoko Belt into three tectonic zones. The Eastern Kaoko Zone is a >2 km thick sedimentary succession deposited on top of the cratonic basement represented by pre-Neoproterozoic rocks of the Kamanjab and Epupa inliers (Fig. 1). Neoproterozoic sediments start with quartzites and quartzitic conglomerates of the Nosib Group and these are overlain by the Otavi Group carbonate platform. The uppermost unit deposited unconformably on top of the Otavi Group carbonates is the siliciclastic Mulden Group interpreted as molasse sediments with respect to the easterly developing orogenic front (Hoffmann and Prave, 1996; Prave, 1996). No absolute age estimates for the particular members of the Eastern Kaoko Zone sediments are available but they can be correlated with corresponding strata in the Otavi Platform. The Central Kaoko Zone is thrust over the Eastern Zone along a westerly dipping low-angle Sesfontein Thrust. The Central Zone consists of a pile of metasediments on top of, or interleaved with, basement rocks of the Congo Craton. The metamorphic grade increases from greenschist-facies in the east up to lower granulite-facies conditions in the west (Franz et al., 1999; Goscombe et al., 2003b; Will et al., 2004). The Western Kaoko Zone of Miller (1983) has been subdivided into two tectonic units by Goscombe et al. (2005). The easterly Orogen Core unit is in contact with the Central Kaoko Zone along a large-scale transpressional Purros Shear Zone (Fig. 2) and consists of slivers of the pre-Neoproterozoic basement rocks intercalated with metasediments of unknown age. The whole unit has been metamorphosed under granulite-facies conditions at c. 550 Ma (Goscombe et al., 2005; Konopásek et al., 2005, 2008). The westernmost part of the Western Kaoko Zone is represented by the Coastal Terrane built of amphibolite-/granulite-facies metasedimentary rocks (Goscombe et al., 2005; Goscombe and Gray, 2007) metamorphosed at c. 650–630 Ma (Franz et al., 1999; Goscombe et al., 2005; Konopásek et al., 2008) and intruded by numerous granitoid rocks with intrusion ages spanning a period between c. 800 Ma and 550 Ma (Seth et al., 1998; Kröner et al., 2004; Masberg et al., 2005; Konopásek et al., 2008; Janoušek et al., 2010). No pre-Neoproterozoic rocks have been reported from this unit. Due to the c. 100 My difference in the timing of the metamorphic peak, lack of pre-Neoproterozoic basement and apparently distinct geochemistry and isotopic signatures of the metasediments, the Coastal Terrane has been interpreted by Goscombe and Gray (2007) as an arc/back-arc-type terrain with pre-collisional tectonic evolution independent of that along the Congo Craton passive margin. Dating of metamorphism in the Central Kaoko Zone and in the Orogen Core suggests that the Coastal Terrane collided with the western Congo Craton margin between c. 575–565 and 550 Ma (Goscombe et al., 2003b, 2005; Jung et al., 2007; Konopásek et al., 2008; Ulrich et al., 2011). The Coastal Terrane has been recently correlated with the Punta del Este Terrane of the Dom Feliciano Belt in eastern Uruguay due to the similarities in the timing of magmatic and metamorphic events in these two units (Gross et al., 2009; Oyhantçabal et al., 2009; Lenz et al., 2011).

The western part of the Central Kaoko Zone, the Orogen Core and the Coastal Terrane units, which are the subject of this paper, underwent amphibolite- to granulite-facies metamorphism and intense deformation

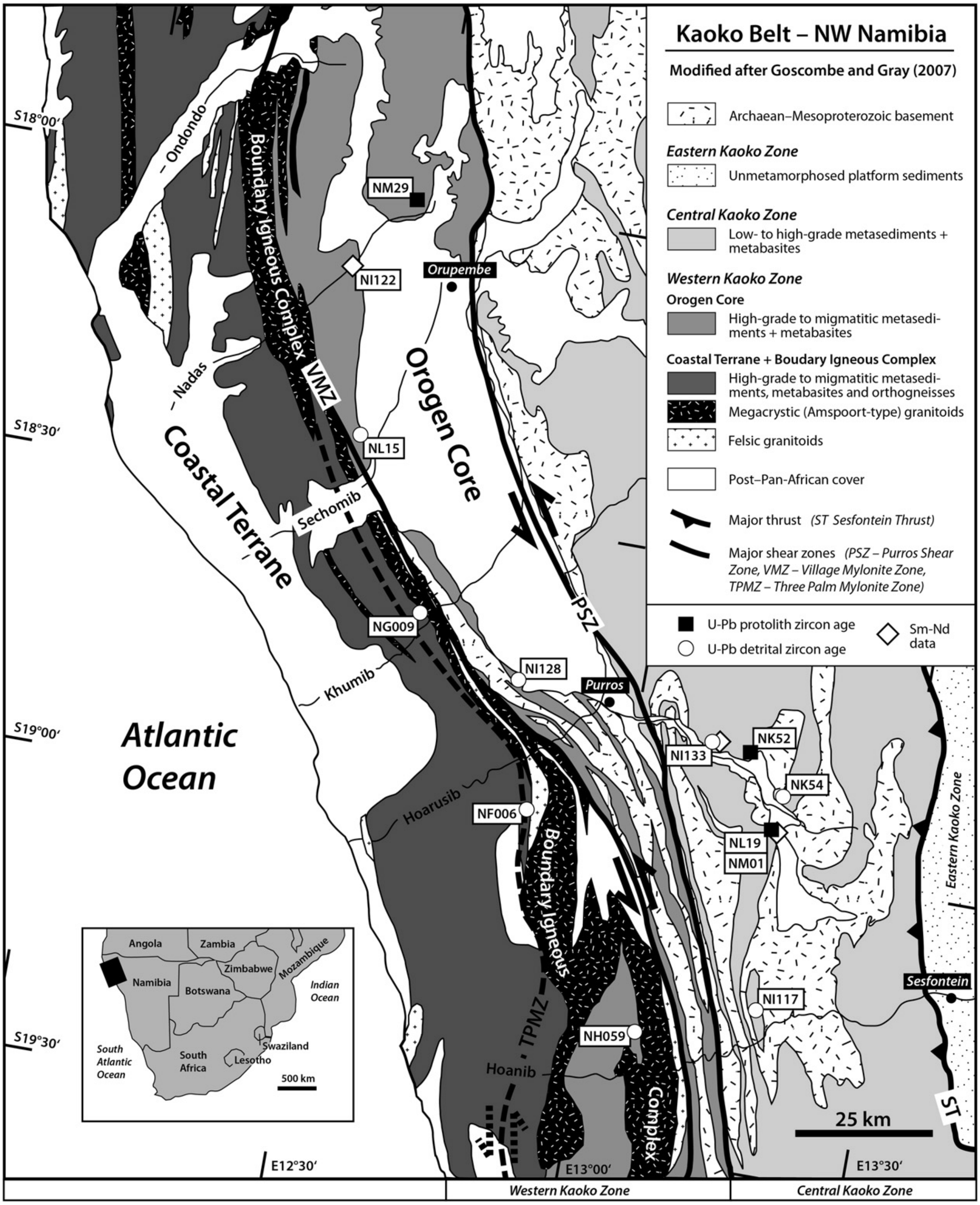

Fig. 2. Simplified geological map of the Kaoko Belt (modified after Goscombe and Gray, 2007) with the locations of the studied samples.

which makes it difficult to correlate the metasediments with non-metamorphosed sedimentary sequences of the Congo Craton passive margin. Guj (1970) did not recognize any pre-Neoproterozoic basement in these units and assigned all the metamorphic rocks west of the Sesfontein Thrust to the Neoproterozoic pre-orogenic sedimentary cover. Dingeldey et al. (1994) interpreted the metasediments in the western part of the Central Kaoko Zone and in the Orogen Core unit as metamorphosed equivalents of the upper part of the Swakop Group, i.e. the interval between c. 630 and 580 Ma according to the chronostratigraphic table of Hoffmann et al. (2004), and the majority of the Coastal Terrane as the pre-Damaran basement. Goscombe (1998a,b) published two 1:50 000 geological map sheets that re-interpreted a large part of an area mapped by Guj (1970) by recognizing the presence of the pre-Damara gneissic basement underlying the metamorphosed Damara sediments. In the Goscombe's (1998a,b) interpretation, the lowermost Damaran Nosib Group sediments appear only in the eastern part of the Central

Kaoko Zone and most of the metasediments represent the former deep basin and slope facies of the Swakop Group (the interval of c. 730–650 Ma in Goscombe, 1998a,b). According to Goscombe and Gray (2008), the northern part of the Orogen Core unit contains distinct siliciclastic suite of metamorphosed quartzites and arkoses that may represent an intra-orogen molasse equivalent to the Mulden Group (i.e. <c. 580 Ma according to Hoffmann et al., 2004).

3. Central Kaoko Zone — description of samples and results of U–Pb zircon dating

U–Pb ages of detrital zircon populations in metasedimentary samples were determined by laser ablation inductively coupled plasma mass spectrometry (LA-ICP-MS). Reported zircon U–Pb concordia age spectra comprise only analyses with 2σ uncertainty $\leq$10% and probability of concordance $\geq$1%. Dating of zircon from metavolcanic samples was carried out by secondary ion mass spectrometry (SIMS) and/or LA-ICP-MS and all reported uncertainties are 2σ. Description of zircon separation and particular analytical methods is provided in the Appendix A. The frequency of zircon age populations is presented in the form of histograms and kernel function described in Vermeesch (2012). All isotopic data are given in the electronic appendix.

3.1. Sample NL 19: amphibolite from the Central Kaoko Zone

Sample NL 19 (S18°48.437′, E13°05.704′ — all coordinates are WGS 84) is medium-grained plagioclase-rich amphibolite (Fig. 3a) surrounded by prevailing dark, amphibole-rich variety that appears as thick layers in the metasedimentary unit of the western part of the Central Kaoko Zone (Fig. 2). The light amphibolite contains metamorphic mineral assemblage plagioclase–quartz–amphibole–epidote–garnet–opaque mineral typical of the lower/middle amphibolite-facies conditions. No temporal relationship between the two amphibolite varieties could be assessed due to intense deformation and metamorphism and we interpret the sampled plagioclase-rich type as an intermediate member of a former predominantly mafic lava or ash flow.

The sample NL 19 is rich in c. 100–150 μm long zircon with well preserved prismatic crystal faces. Zircon crystals contain inclusions of quartz and show oscillatory zoning in the CL (Fig. 3a). LA-ICP-MS dating of these zircons yielded a pooled concordia age of 730 $\pm$ 4 Ma (Fig. 3b). SIMS dating provided a single cluster of data that combined in a concordia age of 735 $\pm$ 4 Ma (Fig. 3c). The age of 735–730 Ma is interpreted as the timing of zircon crystallization from the magmatic protolith of the amphibolite.

3.2. Sample NK 52: clinozoisite-rich lenses in amphibolite of the Central Kaoko Zone

Sample NK 52 (S18°48.437′, E13°05.704′) comes from a thick layer of amphibolite in the eastern limb of a large synformal structure in the western part of the Central Kaoko Zone (Fig. 2) metamorphosed in the lower amphibolite facies (Goscombe et al., 2003b; Will et al., 2004). The main body of amphibolite contains 2–10 cm thick lenses and layers of light colored to white rocks (Fig. 3d) that are interpreted as metamorphosed aluminium-rich and Fe–Mg-poor ash or lava layers within a body of mafic volcanics. Majority of the rock is a fine grained aggregate of clinozoisite in assemblage with subordinate amphibole, titanite, plagioclase and $\pm$quartz.

The sample contains highly corroded, up to 200 μm long prismatic zircon grains with relics of crystal faces. The crystals are dark in CL with traces of zoning, they all show bright rims and occasionally also CL-bright inner domains, perhaps due to the interaction with metamorphic fluids (Fig. 3d). LA-ICP-MS dating of the CL-dark interiors of these zircons yielded one major cluster of data and three analyses falling outside of this main cluster (not shown on the concordia diagram in Fig. 3e). The pooled concordia age calculated for the main cluster of data is 738 $\pm$ 7 Ma (Fig. 3e). SIMS dating provided one cluster of concordant data and five concordant or discordant analyses that plot away from the main cluster. The two analyses suggesting an older age than that for the main cluster are difficult to interpret, the three concordant analyses that provided younger ages possibly refer to some Pb-loss in the time of metamorphism at 575–550 Ma. These data (see the electronic appendix) are not shown on the concordia diagram in Fig. 3f. The main cluster of data yielded a concordia age of 739 $\pm$ 5 Ma (Fig. 3f) that corresponds well to the LA-ICP-MS age and we interpret it as the best estimate of the timing of zircon crystallization in the magmatic protolith of the amphibolite.

3.3. Sample NK 54: quartzite of the Central Kaoko Zone

Sample NK 54 (S18°53.362′, E13°17.698′) is muscovite- and biotite-bearing quartzite collected from a c. 20 cm thick layer that appears structurally immediately below the amphibolite layer containing the sample NL 19 (Fig. 2). According to the geological map of Goscombe (1998b) and an interpretative profile given in Goscombe et al. (2003a), the rock assemblage in this location represents a western limb of an overturned synform and thus prior to the folding the NK 54 quartzite appeared structurally above the NL 19 amphibolite.

The morphology of zircon in this sample ranges from completely rounded grains with no relics of crystal faces through partly rounded hypidiomorphic to idiomorphic prismatic grains. Cathodoluminescence images of their internal structures show mostly oscillatory growth zoning, sometimes truncated at the edges of the grains, probably as a result of abrasion during the transport. Some grains have up to 10 μm wide bright overgrowths on the oscillatory-zoned cores. U–Pb dating by LA-ICP-MS yielded data with probability of concordance $\geq$1% and 2σ uncertainty $\leq$10% for 74 zircon grains. The resulting data are presented in Fig. 4a and the corresponding age spectrum shows two main peaks at c. 1.40 Ga and c. 1.85 Ga, where the latter overlaps with another peak at c. 2.00 Ga.

3.4. Sample NI 133: biotite schist of the Central Kaoko Zone

Sample NI 133 (S18°49.283′, E13°08.314′) comes from a metasedimentary unit overlying the Congo Craton basement gneisses in the Central Kaoko Zone (Fig. 2). The rock is fine-grained biotite schist consisting of quartz, plagioclase, biotite and carbonate. In the geological map of Goscombe (1998b) and in the profile given in Goscombe et al. (2003a) the sample is located in the structurally uppermost part of the metasedimentary pile of the Omapungwe synform in the Gomatum Valley section.

The majority of the zircon extracted from this sample is grain fragments showing no crystal faces and only small proportion of the grains have short prismatic crystal shapes. Cathodoluminescence imaging revealed truncated oscillatory zoning in majority of the grains. Most show very thin overgrowths or small embayments into the original oscillatory zoning of the crystals that may be indicative of a period of zircon recrystallization or new growth. Analyses of 62 grains provided data with probability of concordance $\geq$1% and 2σ uncertainty $\leq$10%. The spectrum of concordia ages is presented in Fig. 4b and shows two large peaks at c. 750 Ma and c. 1.00 Ga and individual data at c. 650 Ma, 1.18 Ga and 1.80 Ga.

3.5. Sample NI 117: quartzite of the Central Kaoko Zone

Sample NI 117 (S19°15.568′, E13°18.916′) is a metamorphosed arkosic quartzite interpreted as an equivalent of the basal Nosib Group sediments collected in a structure known as the Obias Tectonic Window (Fig. 2; Guj, 1970; Dingeldey et al., 1994). The sample contains quartz, plagioclase, microcline and white mica with subordinate biotite, tourmaline and opaque mineral.

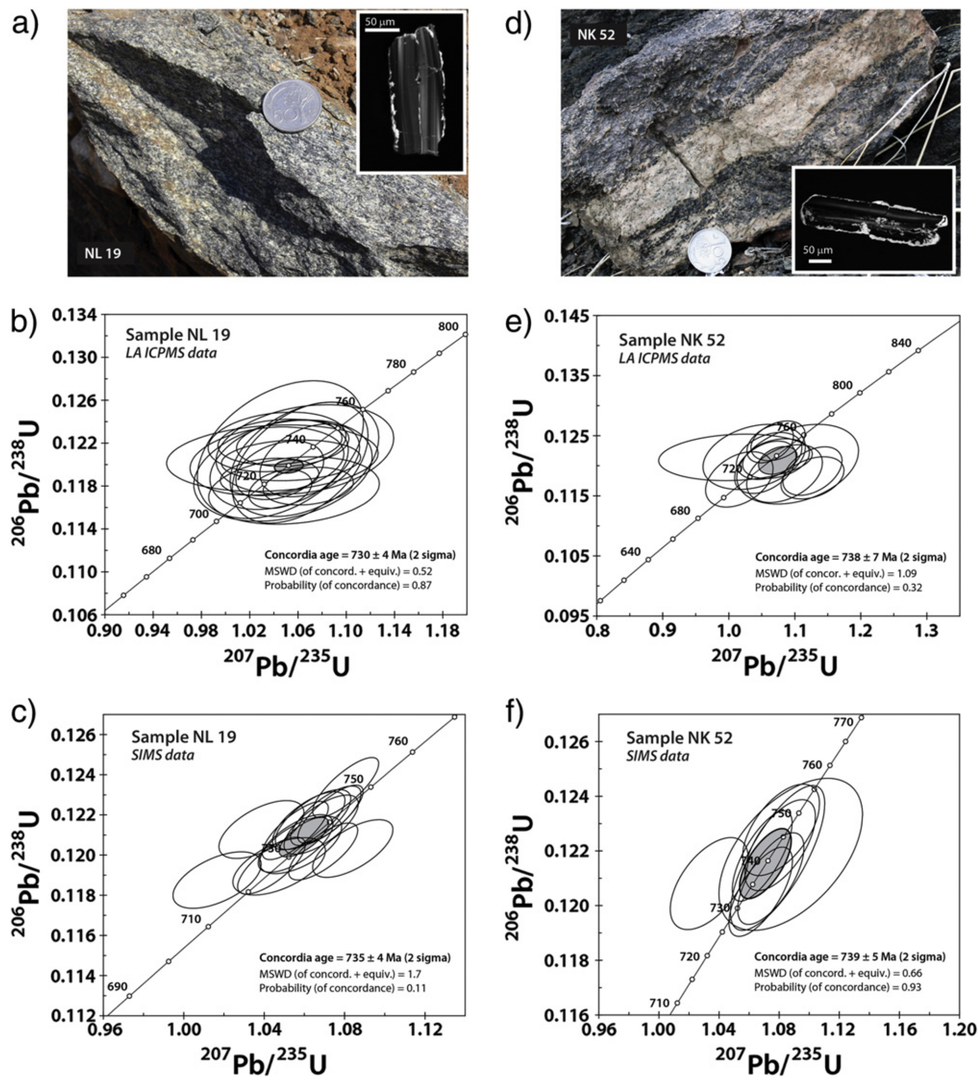

Fig. 3. Field appearance (a and d) and the results of the isotopic age determinations (b, c, e and f) of the samples NL 19 and NK 52. Cathodoluminescence images of typical zircon grains from the respective samples are shown as insets in figures a) and d).

Zircon grains are mostly rounded, some are prismatic but often with rounded edges of the crystal faces. Cathodoluminescence images of the rounded crystals often show truncated oscillatory zoning typical of mechanically abraded detrital grains. Analysis of 88 grains provided data with probability of concordance $\geq 1\%$ and 2σ uncertainty of $\leq 10\%$. The corresponding age spectrum is presented in Fig. 4c and shows one broad composite peak centered at c. 2.00 Ga, another peak at c. 1.25 Ga and individual data around 1.05, 1.5 and 1.7 and between 2.6 and 2.9 Ga.

4. Western Kaoko Zone — description of samples and results of U–Pb zircon dating

4.1. Sample NM 29: quartz-feldspathic layer in amphibolite of the Orogen Core

Sample NM 29 (S18°00.726′, E12°27.088′) comes from a prominent horizon of amphibolite that forms several km wide fold structure visible in the satellite images and located c. 20 km NNW of the settlement of Orupembe (Fig. 2). The amphibolite body is part of the Orogen Core unit and the metamorphism of surrounding metasediments reached the conditions of the upper amphibolite-/granulite-facies transition. We have sampled c. 0.5 m thick, continuous layer of quartz-feldspathic rock (Fig. 5a) that is developed in the eastern limb of the folded amphibolite body. The rock is made of ribbons rich in quartz alternating with bands rich in both plagioclase and K-feldspar. It contains partly chloritized biotite with needle-like crystals of rutile and opaque minerals. We interpret this sample as metamorphosed silica-rich ash or lava layer within a mafic volcanic body.

Zircon in this sample is short prismatic either with oscillatory or hourglass sector zoning (Fig. 5a). Its dating by SIMS yielded a cluster of concordant analyses that combine in a concordia age of 708 ± 3 Ma (Fig. 5b). Four other data plot on the concordia away from the main cluster and give younger ages (data in electronic appendix). These data (not shown on the concordia diagram in Fig. 5b) are interpreted as originating from Pb-loss, possibly during metamorphism at 575–550 Ma. The concordia age of 708 ± 3 Ma is interpreted as the crystallization age of the sample protolith.

4.2. Sample NI 128: quartzitic gneiss of the Orogen Core unit

Sample NI 128 (S18°46.077′, E12°46.725′) comes from metasedimentary unit that overlies the Paleo–Mesoproterozoic basement gneisses (Kröner et al., 2004) in the southern part of the granulite-

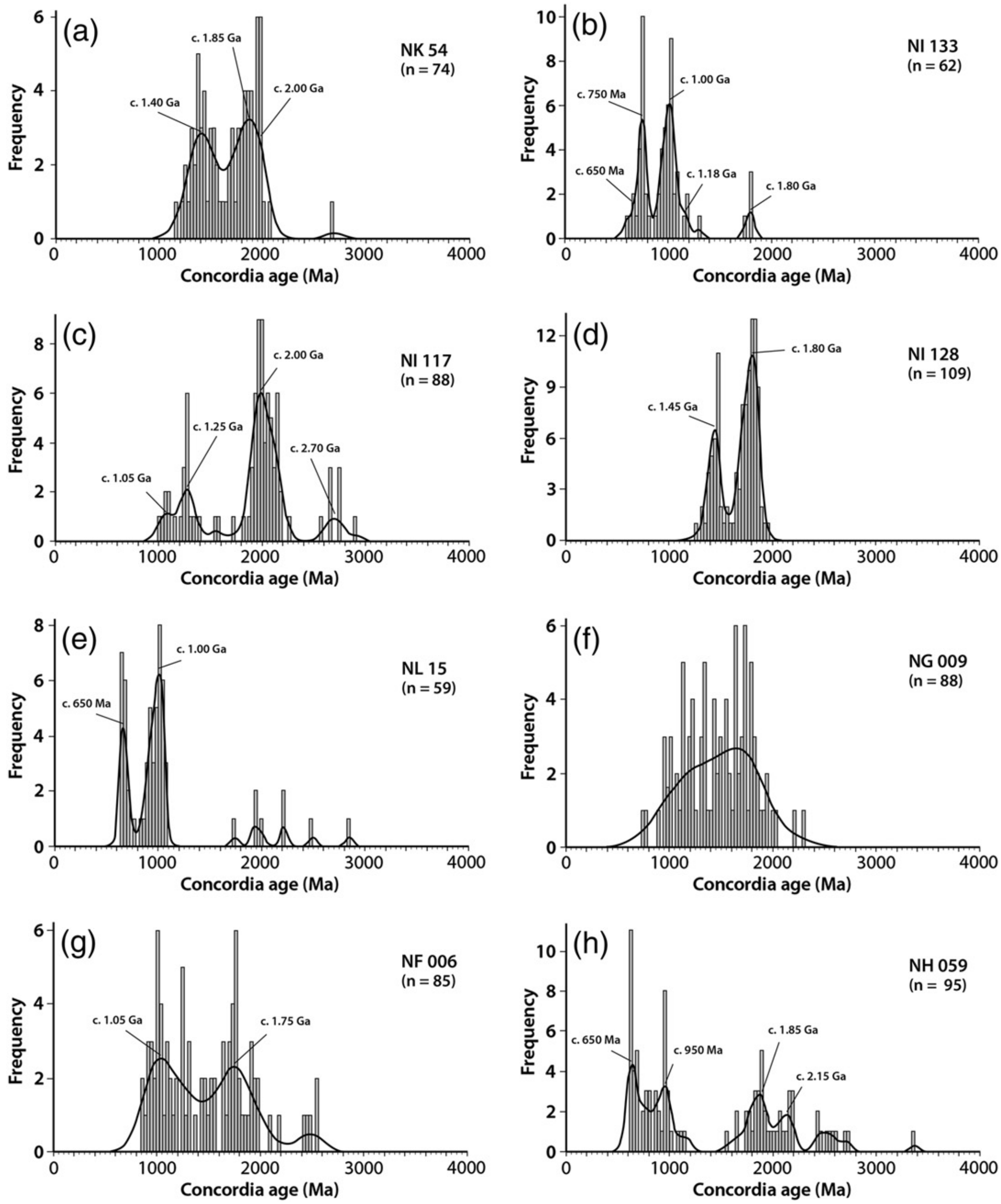

Fig. 4. Detrital zircon age data for metasedimentary samples from the Central Kaoko Zone (a–c) and the Western Kaoko Zone (d–h).

facies Orogen Core unit (Fig. 2). The dated rock is quartzitic gneiss consisting predominantly of quartz associated with K-feldspar, plagioclase, biotite and small amount of garnet. The zircon population shows mostly rounded grains, although some hypidiomorphic crystals are also present. Cathodoluminescence images of the measured zircon grains often show truncated oscillatory zoning and many grains have thin recrystallized or newly-grown rims.

Analysis of 109 grains provided data with probability of concordance $\geq 1\%$ and 2σ uncertainty of $\leq 10\%$. These ages cluster around two peaks at c. 1.45 and 1.80 Ga (Fig. 4d).

4.3. Sample NL 15: quartzitic gneiss of the Orogen Core unit

This sample (S18°24.985′, E12°26.633′) represents a quartzitic layer from metamorphosed sequence of regularly alternating quartzites and metapelites north of the Sechomib river valley (Fig. 2). The rock sample consists mostly of quartz together with plagioclase, carbonate, garnet, clinopyroxene, clinoamphibole and secondary clinozoisite. Zircon grains from this sample are mostly prismatic, sometimes with rounded edges of the crystal faces. Cathodoluminescence images show that the majority of crystals have well developed oscillatory zoning and several microns thick newly grown or recrystallized rims.

Analyses of 60 grains yielded data with probability of concordance $\geq 1\%$ and 2σ uncertainty of $\leq 10\%$. One grain gave a concordia age of 549 ± 41 Ma (2σ). As this is the age of migmatization in the Orogen Core unit, the dated grain is interpreted as being metamorphic. Remaining data show age peaks at c. 650 Ma and 1.00 Ga and individual data between c. 1.75 and 2.85 Ga (Fig. 4e).

4.4. Sample NG 009

Sample NG 009 (S18°40.470′, E12°35.755′) was collected in a zone of strongly sheared metasediments adjacent to deformed granitoids of the Boundary Igneous Complex (Fig. 2). The sample is almost pure

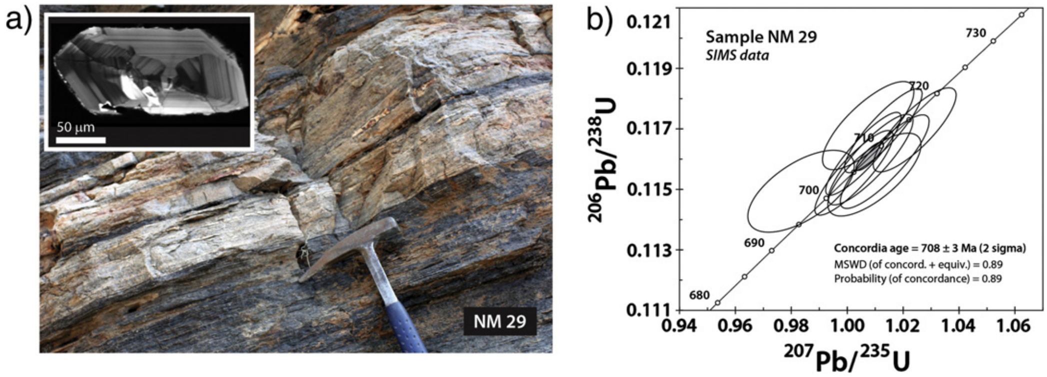

Fig. 5. Field appearance (a) and the result of the SIMS isotopic age determination (b) of the sample NM 29. Cathodoluminescence image of typical zircon grain from the sample is shown as inset in figure (a).

quartzite with subordinate plagioclase, biotite and sillimanite. Majority of the zircon grains are rounded and only few show relics of crystal faces. Cathodoluminescence images show often truncated oscillatory or sector zoning; some grains contain older weakly zoned cores overgrown by oscillatory-zoned rims and several have only faint or no zoning. Some grains show thin overgrowths or zones of recrystallization at the rims.

Analysis of 90 grains provided isotopic ratios with probability of concordance ≥1% and 2σ uncertainty of ≤10%. Two concordia ages (573 ± 58 and 619 ± 62 Ma; 2σ) were obtained by dating of zircon overgrowths and these are not considered as analyses of detrital grains. The distribution of calculated ages for remaining 88 grains is presented in Fig. 4f that shows a range of data in the interval between c. 900 Ma and 2.00 Ga, and some individual data at c. 750 Ma, 2.20 Ga and 2.30 Ga.

4.5. Sample NF 006: quartzite of the Coastal Terrane

Sample NF 006 (S18°57.995′, E12°52.563′) comes from a metasedimentary unit on top of the Boundary Igneous Complex (Fig. 2) and also structurally above the main body of felsic and mafic magmatic rocks emplaced at c. 800 Ma and metamorphosed under the granulite facies at c. 650–630 Ma (Konopásek et al., 2008). The sample is a coarse-grained quartzite, in which quartz is accompanied by biotite and low amount of plagioclase and K-feldspar. The population of zircons is very similar to that in sample NG 009 and the only difference is the apparently higher number of elongate grains with visible relics of crystal faces in sample NF 006. Cathodoluminescence imaging shows features identical to the sample NG 009.

U–Pb dating of 96 zircon grains yielded data with probability of concordance ≥1% and 2σ uncertainty of ≤10%. Out of these, 11 analyses were made from overgrowths of crystal cores and these provided single grain concordia ages in the range of 727–617 Ma. The remaining 85 data were considered as representing detrital grains and their corresponding calculated ages range between c. 850 Ma and 2.00 Ga with two peaks at c. 1.05 Ga and 1.75 Ga, and also some individual data between c. 2.10 and 2.20 Ga and between c. 2.40 and 2.60 Ga (Fig. 4g).

4.6. Sample NH 059

Sample NH 059 (S19°16.279′, E13°05.286′) is an impure quartzite that crops out in the unit of metasediments within the southernmost part of the Boundary Igneous Complex. The metasediments are metamorphosed under the granulite-facies conditions and the quartzite sample contains the mineral assemblage quartz, plagioclase, clinopyroxene, amphibole, titanite and carbonate. Zircon grains are often short prismatic, some of them isometric. Cathodoluminescence images reveal that in many cases the tips of the prismatic grains are represented by sector- or, less frequently, oscillatory-zoned overgrowths of rounded cores with variable zoning patterns.

The U–Pb analyses of 104 zircon grains yielded data with probability of concordance ≥1% and 2σ uncertainty of ≤10%. Nine analyses of core overgrowths provided single grain concordia ages in the range of 603–539 Ma and a pooled concordia age of 558 ± 13 Ma (2σ). The rest of the data was considered as representing detrital grains and their calculated ages show peaks at c. 650 Ma, 950 Ma, 1.85 Ga and 2.15 Ga, individual ages between c. 2.40 and 2.75 Ga and one age of c. 3.35 Ga (Fig. 4h).

5. Discussion

5.1. Age of volcanic activity in the Central Kaoko Zone and in Orogen Core unit

The sample of metamorphosed felsic volcanic rock NM 29 from the Orogen Core unit yielded an age of c. 710 Ma and dating of samples NL 19 and NK 52 from prominent amphibolite layers exposed in the Central Kaoko Zone has provided ages of c. 735–730 and c. 740 Ma, respectively. According to the geological maps of Goscombe (1998a,b), the dated samples from the Central Kaoko Zone lie within metasedimentary rocks close to the gneissic basement and provide first robust information about the age of early syn-sedimentary volcanic activity in the Kaoko Belt. The reported ages from the Central Kaoko Zone samples are similar to, though somehow younger than, the timing of the early magmatic activity in the Damara Belt, where the ages of 756 and 746 Ma by Hoffman et al. (1996) provide the upper limit for the timing of sedimentation of the rifting-related clastics of the Nosib Group. Our data suggest c. 15–25 Ma delay in the syn-rifting magmatic activity along the southern and western margin of the southwestern tip of the Congo Craton.

5.2. Age of sedimentation in the Central and Western Kaoko zones

Detrital zircon data (Fig. 4) can be separated into three groups based on both the geotectonic setting of sampled rocks and resulting age spectra. The first group is represented by samples NI 133, NL 15 and NH 059 that were collected from the metasedimentary cover of the Congo Craton basement and contain Neoproterozoic zircons with ages between c. 800 and 650 Ma (Fig. 4b, e, h). Even the youngest zircons in the granulite-facies samples NH 059 and NL 15 are oscillatory zoned which points to their magmatic rather than metamorphic origin. The samples of this group also show a marked peak at c. 1.00 Ga and subordinate number of zircons older than c. 1.2 Ga. The youngest peak of detrital zircon ages at c. 650 Ma and the age of early metamorphism in the Kaoko Belt determined by Goscombe et al. (2003b) and Jung et al. (2007) at c. 575–565 Ma suggest that the sedimentary precursor must have been deposited between c. 650 and c. 570 Ma. The field relationships suggest that all the samples of this group come from locations that are, in terms of effective thickness, distant from the Congo Craton gneissic basement and thus very likely represent stratigraphically higher parts of the preserved Neoproterozoic sedimentary strata in the study region (Fig. 6).

Second group of samples (NK 54, NI 117 and NI 128) comes from localities where the effective distance from the Congo Craton basement is small (Fig. 6) and the rocks thus probably represent the bottom of the pre-collisional Neoproterozoic sedimentary cover. These samples contain only Mesoproterozoic and older zircons with majority of ages concentrated in the time interval between c. 1.00 and 2.20 Ga (Fig. 4a, c, d). The distribution of detrital zircon ages is almost identical in the samples NK 54 and NI 128 (Fig. 4a, d), whereas the sample NI 117 contains significant number of zircons with ages between c. 1.00 and 1.25 Ga, which are missing (or are only marginally present) in samples NK 54 and NI 128.

The youngest clastic zircons in sample NI 117 of the second group cluster around c. 1.00 Ga, which is a good evidence for the Neoproterozoic age of the sedimentary precursor. The youngest zircons in NI 128 and NK 54 are older (peak around 1.45–1.40 Ga) and their Neoproterozoic age thus cannot be confirmed by detrital zircon ages. However, dating of the intermediate–mafic metavolcanic sample NL 19 situated originally (prior to folding) below the quartzite sample NK 54 provided the protolith age of 735–730 Ma, suggesting also a maximum sedimentary age for the sample NK 54. Samples NI 117, NI 128 and NK 54 were collected in the close proximity of the basement metagranitoids and it is thus likely that, with respect to the above-discussed first group of samples, the second group represents stratigraphically lower parts of the Neoproterozoic Congo Craton cover (Fig. 6).

The third group represents samples NG 009 and NF 006 collected in the hanging wall of the Boundary Igneous Complex where the rocks according to our earlier interpretation (Konopásek et al., 2008) represent the Coastal Terrane metasediments. These two samples thus represent tectonically the lowermost part of the Coastal Terrane that is overlain by biotite- and amphibole-bearing gneisses interpreted by Goscombe and Gray (2007) as metamorphosed arc-related sediments (Fig. 6). They show almost equal distribution of zircon ages between c. 900 Ma and c. 2.00 Ga accompanied by some individual older grains (Fig. 4f, g). In the sample NG 009 we have also encountered two c. 750 Ma old zircons. These data also suggest Neoproterozoic age of sedimentation for this part of the Coastal Terrane. The age of the sedimentation is, however, bracketed also by the c. 800 Ma age of underlying bimodal metaigneous rocks and by the age of metamorphism of the Coastal Terrane at c. 650 Ma (Konopásek et al., 2008).

5.3. Comparison with existing detrital zircon data

The only available detrital zircon data for (meta)sedimentary rocks from similar tectonic setting come from the northern Kaoko Belt, the Gariep Belt in southern Namibia and from one sample of the basal Nosib Group in the Damara Belt. The data from the Hartmann Group in the northern Kaoko Belt (sample NK91 of Goscombe et al., 2005) show very good match with our sample NI 117 (Fig. 4c), except that

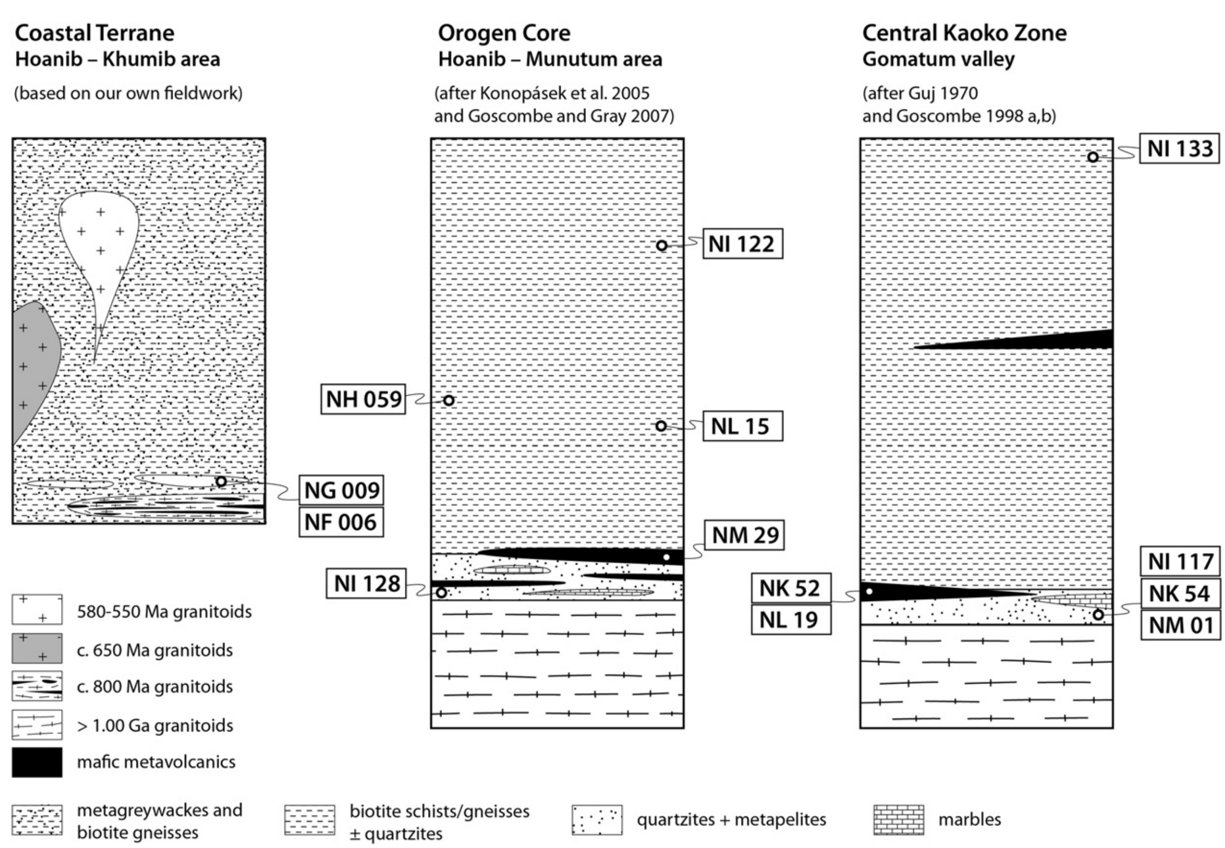

Fig. 6. Schematic interpretation of tectonostratigraphic position of the samples from this study. Presented lithological successions for the particular geological units of the Kaoko Belt represent compilations from the various maps presented by Guj (1970), Goscombe (1998 a,b), Konopásek et al. (2005), and Goscombe and Gray (2007) and from our own mapping. The thickness of various lithologies is not to scale.

we have not observed the c. 1.75 Ga peak. This similarity suggests that the Hartmann Group quartzites should be correlated with the Nosib (c. 800–750 Ma) quartzite exposed in the Obias river window (sample NI 117) rather than with an intra-orogenic molasse as suggested by Goscombe and Gray (2008).

The detrital zircon data from the Gariep and Damara belts (Basei et al., 2005, 2008) are also comparable with our results, even though the authors provide only ages for small number of zircons from each sample. The basal sediments (Nosib Group of the Damara Belt and Stinkfontein Subgroup in the Gariep Belt) show a range of ages between c. 1.00 and 2.00 Ga and thus match well our data from the lowermost part of the Neoproterozoic cover sequence in the Kaoko Belt (cf. fig. 9 in Basei et al., 2008 and Fig. 4b in this paper). The sample from the upper part of the sedimentary succession in the Gariep Belt (the Oranjemund Formation) shows an age pattern that matches zircon ages in our samples from the upper part of the Kaoko cover sequence, i.e. maxima at c. 650 Ma and c. 1.00 Ga and limited number of Paleoproterozoic zircons (cf. fig. 9 in Basei et al., 2008 and Fig. 4a in this work). However, more detailed comparative study with higher number of analyzed zircon grains is needed for making a more conclusive correlation of the sedimentary evolution in the Kaoko and Gariep belts.

5.4. Possible sources of clastic sediments deposited along the western Congo Craton margin

Tectonic reconstructions of the pre-collisional evolution in the Kaoko–Damara–Gariep–Dom Feliciano belts (Miller, 1983; Porada, 1989; Goscombe and Gray, 2007; Frimmel et al., 2011) suggest four possible source regions for the original detrital material of the studied metasedimentary samples. The most likely source region, especially for the early Neoproterozoic sedimentation in the Kaoko Belt, is represented by the granitoids and pre-Neoproterozoic metasediments of the Congo Craton. Moreover, inferred relatively small separation of the Congo and Kalahari cratonic blocks at the end of the rifting/break-up period (e.g. Miller, 1983; Frimmel et al., 2011) suggests that the Kalahari Craton could have acted as another source of detritus for the early sedimentation along the south-western Congo Craton margin.

Our data show that the sedimentation age of at least three samples is undoubtedly younger than c. 650 Ma. The presence of zircon grains with these ages implies that detrital material from post-rifting, but pre-collisional Neoproterozoic granitoids was also present in the studied metasediments. Goscombe and Gray (2007, 2008) have suggested that the apparently exotic Neoproterozoic Coastal Terrane may have not been separated from the Congo Craton margin by an extensive oceanic domain prior to their mutual collision during the late Neoproterozoic. The tectonic evolution of the Coastal Terrane was recently correlated with that of the Punta del Este Terrane in the easternmost part of the Dom Feliciano Belt in Uruguay (Gross et al., 2009; Oyhantçabal et al., 2009; Lenz et al., 2011). We suggest that the Punta del Este – Coastal Terrane may represent another source region for the detrital material deposited along the south-western margin of the Congo Craton.

Finally, there is a large volume of felsic igneous rocks that have originated during Neoproterozoic early rifting between the Congo and the Kalahari cratons (Miller, 1983) dated by Hoffman et al. (1996) and Halverson et al. (2005) at 760–746 Ma. In the upper part of the stratigraphic interval, locally developed predominantly mafic volcanics with an age close to c. 635 Ma are known from the basinal part of the Neoproterozoic sedimentary succession (Hoffmann et al., 2004) in the Damara Belt. However, all areas with recognized Neoproterozoic igneous activity have probably experienced continuous subsidence up to the commencement of collisional processes in the Kaoko and Damara belts, because there is no evidence for major erosion prior to the onset of discordant sedimentation of molasse-type sediments at c. 580 Ma (Hoffmann and Prave, 1996; Hoffmann et al., 2004). For this reason the Neoproterozoic sedimentary succession with the local presence of igneous rocks is not considered as a possible source region for the protoliths of studied rocks.

Granitoid rocks of the Congo Craton exposures in Namibia have been extensively dated by Seth et al. (1998, 2003), Kröner et al. (2004), Kröner et al. (2010) and Luft et al. (2011). The results show Archean and Paleo- to Mesoproterozoic ages with maxima around c. 1.50, 1.67, 1.77, 1.97 and 2.60 Ga. Zircon ages of granitoids representing the western and northern flanks of the Kalahari Craton in Namibia were reviewed by Becker et al. (2006) and several protolith ages are also known from exposures and drill cores into the northern margin of the Kalahari Craton in Botswana (Singletary et al., 2003). The data show a continuous range of ages between c. 900 Ma and 1.40 Ga with the highest number at c. 1.10 Ga, and also some individual data at c. 1.75 Ga and between 1.87 and 2.05 Ga. The ages of pre-collisional granitoids and migmatitic rocks in the Punta del Este – Coastal Terrane were published by Seth et al. (1998), Franz et al. (1999), Hartmann et al. (2002), Kröner et al. (2004), Goscombe et al. (2005), Konopásek et al. (2008), Oyhantçabal et al. (2009), Lenz et al. (2011) and Masquelin et al. (2012). Their data show two major clusters, one between c. 760 and 800 Ma and the other between c. 630 and 650 Ma. Individual ages of c. 700 and 730 Ma were reported as well. Moreover, Basei et al. (2011), Lenz et al. (2011) and Masquelin et al. (2012) have published ages between c. 920 Ma and 1.20 Ga and some individual data between c. 1.50 and 2.70 Ga for inherited zircon cores. Basei et al. (2011) have suggested that the age of c. 1.00 Ga could be a protolith age for some of the granitoids in the Punta del Este Terrane.

The protolith ages from the potential source regions are presented as bar diagrams in the upper parts of Fig. 7a–c.

5.5. Possible source regions for the studied samples

Pooled data for the samples coming from early cover of the Congo Craton (Fig. 7a) and for those representing upper parts of the metasedimentary pile (Fig. 7b) show distinct difference in detrital zircon age signals.

The data representing the bottom of the Neoproterozoic cover sequence in Fig. 7a were complemented by detrital zircon ages from the sample NK 91 of Goscombe et al. (2005). The samples show mostly Paleo- to Mesoproterozoic detrital zircon ages with two distinct maxima at c. 1.80 and 1.45 Ga, and one maximum at c. 1.95 Ga that overlaps with the peak for the c. 1.80 Ga zircons. All maxima correspond (within uncertainty of a typical U–Pb LA-ICP-MS analysis) well with protolith ages recognized in the Kaoko Belt basement rocks, i.e. the c. 1.97, 1.77 and 1.50 Ga gneisses (Seth et al., 1998, 2003; Kröner et al., 2004, 2010; Luft et al., 2011). The same zircon age groups as those observed in the early sedimentary cover of the Kaoko Belt basement were reported for xenocrystic cores in metamorphic zircon from migmatitic amphibolites in the Orogen Core unit of the Kaoko Belt by Konopásek et al. (2008). The presence of Mesoproterozoic zircons younger than c. 1.50 Ga is difficult to explain, because rocks with such protolith ages have not been so far reported from the Kaoko Belt basement. Perhaps they were present in the upper, now eroded levels of the Congo Craton margin and they do not appear at the present-day basement erosion level. Another possibility is that part of the detritus comes from the Mesoproterozoic Namaqua Metamorphic Complex forming the

Fig. 7. Pooled detrital zircon age data for samples from: a) bottom of the Neoproterozoic sedimentary cover of the Congo Craton (data from this work complemented by those for the sample NK 91 from Goscombe et al. (2005)); b) upper part of the Neoproterozoic metasedimentary cover and c) the tectonically lowermost part of the Coastal Terrane. Upper part of each figure is a bar diagram showing distribution of protolith ages in potential source areas (see text for references).

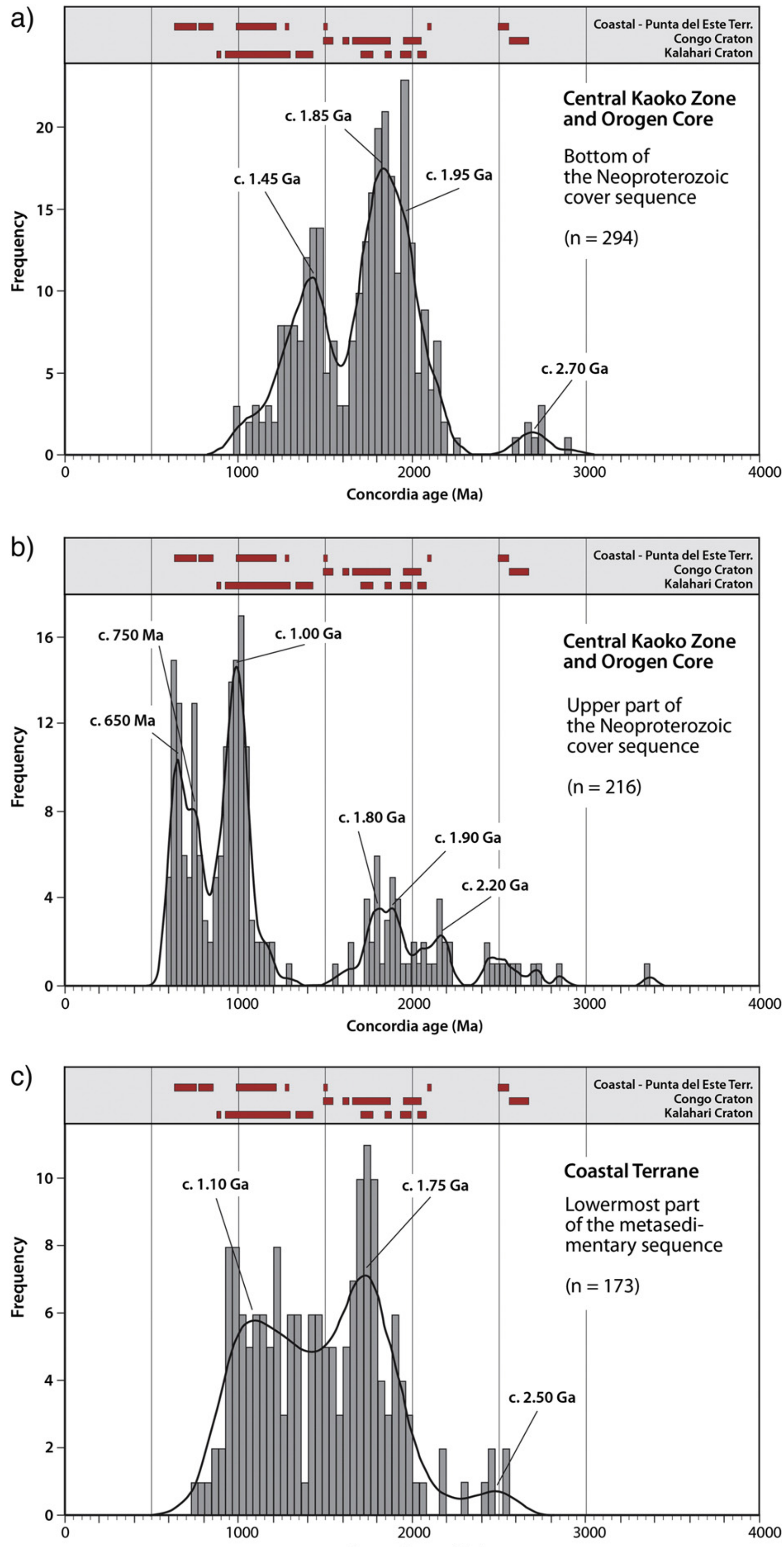
a)
Coastal - Punta del Este Terr.
Congo Craton
Kalahari Craton
Central Kaoko Zone
and Orogen Core
Bottom of
the Neoproterozoic
cover sequence
(n = 294)
c. 1.85 Ga
c. 1.45 Ga
c. 1.95 Ga
c. 2.70 Ga
Frequency
0
5
10
15
20
0
1000
2000
3000
4000
Concordia age (Ma)
b)
Coastal - Punta del Este Terr.
Congo Craton
Kalahari Craton
Central Kaoko Zone
and Orogen Core
Upper part of
the Neoproterozoic
cover sequence
(n = 216)
c. 750 Ma
c. 1.00 Ga
c. 650 Ma
c. 1.80 Ga
c. 1.90 Ga
c. 2.20 Ga
Frequency
0
4
8
12
16
0
1000
2000
3000
4000
Concordia age (Ma)
c)
Coastal - Punta del Este Terr.
Congo Craton
Kalahari Craton
Coastal Terrane
Lowermost part
of the metasedi-
mentary sequence
(n = 173)
c. 1.10 Ga
c. 1.75 Ga
c. 2.50 Ga
Frequency
0
2
4
6
8
10
0
1000
2000
3000
4000
Concordia age (Ma)

western and north-western margins of the present-day Kalahari Craton (Becker et al., 2006), which probably represented one coherent block together with the Congo Craton rocks at the time of the onset of the Neoproterozoic rifting. In any case, the distribution of detrital ages suggests that the source of detritus for the early (i.e. pre-650 Ma) sedimentation must have been the Congo ± Kalahari cratonic basement.

Such interpretation is supported by the two-stage Nd model ages for metasediments from the bottom of the metamorphosed Neoproterozoic cover sequence. Existing data of Goscombe et al. (2005) and Jung et al. (2007) were complemented by an analysis of sample NM 01 (Fig. 8 and Table 1), which is a biotite–muscovite quartzitic gneiss that forms a layer within the dated amphibolite NL 19 and underlies the quartzite NK 54 (Fig. 2). All the Nd model ages for this group of samples fall into interval 2.40–2.12 Ga matching well those for the more juvenile samples of the Congo Craton basement (Fig. 8 inset). This provides another argument that the detritus for the bottom part of the Neoproterozoic cover sequence could have been largely derived from the Congo Craton.

Pooled detrital zircon ages from samples of the upper part of the Neoproterozoic (meta)sedimentary cover (Fig. 7b) suggest important change in the source. Data show rather small proportion of zircons older than c. 1.00 Ga and a dominance of c. 1.00 Ga, c. 750 Ma and c. 650 Ma age groups. Small number of zircons older than c. 1.00 Ga is explained by the fact that in post-650 Ma times, most of the Paleoproterozoic–Archean Congo-Kalahari basement was covered by Neoproterozoic sedimentary succession. Thus, the observed Paleoproterozoic–Archean zircons probably represent the second-cycle grains coming from the source dominated by c. 650 Ma, c. 750 Ma and c. 1.00 Ga rocks. The available protolith ages from various tectonic units of the Kaoko–Damara–Gariep–Dom Feliciano orogenic system suggest that the c. 650 and c. 750 Ma zircons can only come from the Punta del Este – Coastal Terrane. The published protolith ages for the early igneous suite in this unit fall between c. 760 and 800 Ma (U–Pb, SHRIMP; Lenz et al., 2011 or Masquelin et al., 2012) but the distribution of individual data points along the concordia (see diagrams in Lenz et al., 2011 and Masquelin et al., 2012) suggests that ages of detrital zircons derived from such rocks may span a significantly wider time interval. The Coastal Terrane of the Kaoko Belt has been interpreted by Goscombe and Gray (2007) as an arc/back-arc-type terrain with a dominant magmatic activity between c. 650 and 630 Ma and similar protolith ages are known from granitoids of the Punta del Este Terrane and adjacent Granite Belt in Uruguay and southern Brazil (e.g. Babinski et al., 1997; da Silva et al., 1999; Oyhantçabal et al., 2009; Chemale et al., 2012). We suggest that the two above-mentioned igneous suites represent the potential sources of the c. 650 and c. 750 Ma zircons in the post-650 Ma samples. The dominant peak at c. 1.00 Ga remains enigmatic. Several ages close to 1.00 Ga were published for xenocrystic zircon cores in granitoids from the Punta del Este Terrane (Basei et al., 2011; Lenz et al., 2011; Masquelin et al., 2012) and we can only speculate either about mostly eroded or so far unrecognized c. 1.00 Ga old crust in the Punta del Este – Coastal Terrane, or about the presence of important proportion of c. 1.00 Ga zircons in pre-650 Ma (meta)sediments that are associated with the two above-mentioned granitic suites of this tectonic unit.

Existing dataset of Nd isotopic compositions for the samples from the upper part of the Neoproterozoic cover sequence (Goscombe et al., 2003b, 2005) was complemented by analyzing two additional samples. Sample NI 133 has been already described in Section 3.4. Sample NI 122 is a biotite paragneiss that comes from the same unit as the quartzite NL 15. All two-stage neodymium model ages for this group fall in the range 1.82–1.40 Ga (mostly ≤1.5 Ga) and thus they do not overlap with those reported from the Congo Craton basement (Fig. 8 and Table 1). This suggests that substantial portion of the detritus for the upper part of the Neoproterozoic cover sequence must have been derived from a more juvenile crust. On the other hand, the model ages match well the values of the more radiogenic samples of the Coastal Terrane metasediments and metagranitoids (1.78–1.39 Ma, see Table 1), supporting the interpretation that the Coastal Terrane could have been the primary source of detritus for the post-650 Ma sediments along the western margin of the Congo Craton.

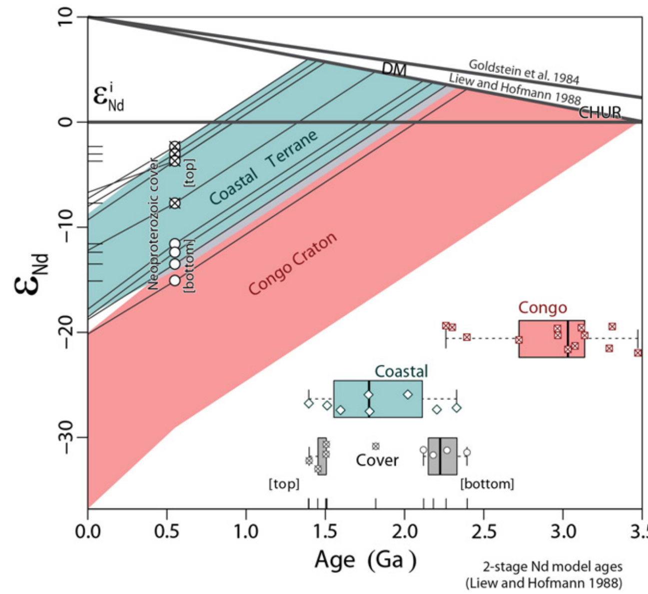

Fig. 8. Two-stage Nd development diagram for metasediments from two stratigraphic levels of the Neoproterozoic cover sequence (Goscombe et al., 2003b, 2005; Jung et al., 2007 and this work). The extra tick marks on the ordinate indicate the initial ε_{Nd} values of the samples, on the abscissa the two-stage Nd Depleted Mantle model ages (Liew and Hofmann, 1988). Composition fields of metasedimentary and metaigneous rocks from Coastal Terrane and Congo Craton (Seth et al., 2002; Goscombe et al., 2003b; Masberg et al., 2005; Seth et al., 2008; Janoušek et al., 2010) are shown for reference. DM = Depleted Mantle evolution lines after Goldstein et al. (1984) and Liew and Hofmann (1988). Inset: 'stripBoxplot' (Janoušek et al., 2006) of two-stage Nd model ages from the same lithologies.

Pooled detrital zircon ages from samples collected in the tectonically lowermost part of the Coastal Terrane (Fig. 7c) show two broad peaks at c. 1.10 Ga and at c. 1.75 Ga, nevertheless the data span the same age interval as those from the basal part of the sedimentary cover of the Congo Craton. Very little is known about the early Neoproterozoic position of the Punta del Este – Coastal Terrane and from the available data it can be only suggested that the source region for the protolith of the dated samples must have had similar protolith ages as the basement of the Congo/Kalahari Craton. It is also possible that the Punta del Este – Coastal Terrane was never separated from the attenuated margin of the Congo Craton.

5.6. Geodynamic implications

The origin of c. 740–710 Ma volcanic rocks intercalating with the sediments derived from the underlying Congo Craton may be correlated with the slightly older syn-rifting magmatism that took place along the southern margin of the Congo Craton in the Damara Belt (Hoffman et al., 1996) and possibly also with the rift-related magmatism of similar age in the Lufilian Arc in Zambia (Key et al., 2001) and in the Tixitonga Basin in Mosambique (Bjerkgard et al., 2009). This suggests that the mantle/lower crustal melting associated with the continental rifting (Fig. 9a) occurred along the entire southern and southwestern part of the Congo Craton between c. 765 and 710 Ma.

Recognition of the Punta del Este – Coastal Terrane as a source of detrital material for the upper part of the Neoproterozoic sedimentary cover of at least a part of the southwestern margin of the Congo Craton suggests that the Punta del Este – Coastal Terrane must have been in close proximity to the Congo Craton margin between c. 650 and 570 Ma, which is

Table 1
Nd isotopic data for samples of the Coastal Terrane, Congo Craton and its metasedimentary cover in the Kaoko Belt. Mean migmatization ages of 550 Ma and 650 Ma were assumed for the Neoproterozoic Cover and Congo Craton and for the Coastal Terrane, respectively.

Sample	Rock type	Unit	Proximal detrital Zrn sample	Metamorphic age (i)	Sm (ppm)	Nd (ppm)	$^{147}Sm/^{144}Nd$	$^{143}Nd/^{144}Nd$ [a]	$^{143}Nd/^{144}Nd_i$	εNd_i	T^{Nd}_{DM} (1stg)	T^{Nd}_{DM} (2stg)	source
NI 122	Bt paragneiss	Neoproterozoic cover — top	NL 15	550 Ma	7.28	34.90	0.1261	0.512265 (11)	0.511811	-2.3	1.45	1.40	This work
NI 133	Bt–Ms schist	Neoproterozoic cover — top	NI 133	550 Ma	5.57	28.10	0.1257	0.512227 (08)	0.511774	-3.0	1.51	1.45	This work
NM 01	Bt–Ms quartzitic gneiss	Neoproterozoic cover — bottom	NK 54	550 Ma	3.64	17.69	0.1246	0.511604 (14)	0.511155	-15.1	2.49	2.40	This work
553	Grt–Bt–Sill gneiss	Neoproterozoic cover — bottom	NI 128	550 Ma	8.13	45.58	0.1078	0.511725 (06)	0.511337	-11.6	1.95	2.12	Jung et al. (2007)
K 209	Grt–Bt–Ms schist	Neoproterozoic cover — bottom	NK 54	550 Ma	9.61	53.46	0.1086	0.511687 (22)	0.511296	-12.4	2.01	2.18	Goscombe et al. (2003b)
K 1336b	Grt–Bt gneiss	Neoproterozoic cover — bottom	NI 128	550 Ma	5.07	25.27	0.1212	0.511675 (20)	0.511238	-13.5	2.29	2.27	Goscombe et al. (2003b)
KK 105f	Grt–Bt–Ms schist	Neoproterozoic cover — top	–	550 Ma	7.43	35.52	0.1166	0.512161 (10)	0.511741	-3.7	1.47	1.50	Goscombe et al. (2003b)
NK 58	Semipelite schist	Neoproterozoic cover — top	NL 15	550 Ma	2.91	11.41	0.1541	0.512295 (20)	0.511740	-3.7	2.00	1.50	Goscombe et al. (2005)
NK 189b	Migmatitic gneiss	Neoproterozoic cover — top	NH 059	550 Ma	12.22	55.73	0.1325	0.512012 (18)	0.511535	-7.7	2.00	1.82	Goscombe et al. (2005)
NI 131	Orthogneiss	Congo Craton		550 Ma	3.36	28.80	0.0738	0.510814 (18)	0.510548	-27.0	2.44	3.32	Janoušek et al. (2010)
NI 132	Orthogneiss	Congo Craton		550 Ma	4.88	31.30	0.0994	0.511575 (11)	0.511217	-13.9	2.00	2.30	Janoušek et al. (2010)
NH 155	Orthogneiss	Congo Craton		550 Ma	8.65	51.20	0.1021	0.511611 (09)	0.511243	-13.4	2.00	2.26	Janoušek et al. (2010)
K 983b	Bt–Ms schist	Congo Craton		550 Ma	10.33	55.91	0.1120	0.511559 (14)	0.511155	-15.1	2.26	2.40	Goscombe et al. (2003b)
BK5a	Dioritic gneiss	Congo Craton		550 Ma	8.38	39.59	0.1280	0.511400 (18)	0.510939	-19.4	2.91	2.73	Seth et al. (2002)
N8a	Diorite–gneiss	Congo Craton		550 Ma	5.73	31.35	0.1105	0.511176 (18)	0.510778	-22.5	2.76	2.97	Seth et al. (2002)
BK445a	Dioritic gneiss	Congo Craton		550 Ma	5.19	32.08	0.0978	0.511016 (02)	0.510664	-24.7	2.67	3.14	Seth et al. (2002)
BK439a	Augengneiss	Congo Craton		550 Ma	15.60	98.67	0.0956	0.511049 (18)	0.510705	-23.9	2.58	3.08	Seth et al. (2002)
BK10a	Layered gneiss	Congo Craton		550 Ma	18.60	130.00	0.0864	0.510752 (14)	0.510441	-29.1	2.74	3.48	Seth et al. (2002)
BK446a	Dioritic gneiss	Congo Craton		550 Ma	18.60	130.00	0.1134	0.511185 (14)	0.510776	-22.5	2.82	2.97	Seth et al. (2002)
BK3a	Dioritic gneiss	Congo Craton		550 Ma	6.74	36.50	0.1116	0.511136 (22)	0.510734	-23.4	2.84	3.04	Seth et al. (2002)
BK29a	Augengneiss	Congo Craton		550 Ma	7.20	44.50	0.0978	0.510913 (18)	0.510561	-26.7	2.80	3.30	Seth et al. (2002)
BK1a	Granitic augengneiss	Congo Craton		550 Ma	5.34	30.32	0.1065	0.511061 (24)	0.510677	-24.5	2.82	3.12	Seth et al. (2002)
NI 123	Bt paragneiss	Coastal Terrane		650 Ma	4.76	24.30	0.1184	0.51199 (10)	0.511486	-6.1	1.76	1.77	Janoušek et al. (2010)
NI 130	Bt paragneiss	Coastal Terrane		650 Ma	10.55	56.50	0.1129	0.512138 (09)	0.511657	-2.8	1.45	1.51	Janoušek et al. (2010)
BK 503a	Granulitic gneiss	Coastal Terrane		650 Ma	6.29	28.00	0.1358	0.511698 (10)	0.511119	-13.3	2.65	2.33	Seth et al. (2008)
BK27a	Metagranodiorite	Coastal Terrane		650 Ma	12.60	71.55	0.1063	0.512186 (18)	0.511733	-1.3	1.30	1.39	Seth et al. (2002)
BK425c	Metagranodiorite	Coastal Terrane		650 Ma	5.29	33.45	0.0956	0.512009 (18)	0.511602	-3.9	1.41	1.60	Seth et al. (2002)
D 13	Migmatitic gneiss	Coastal Terrane		650 Ma	6.57	34.61	0.1147	0.511970 (08)	0.511481	-6.2	1.72	1.78	Masberg et al. (2005)
D 87	Migmatitic gneiss	Coastal Terrane		650 Ma	6.39	35.44	0.1144	0.511689 (06)	0.511202	-11.7	2.12	2.21	Masberg et al. (2005)
D 72	Migmatitic gneiss	Coastal Terrane		650 Ma	6.26	34.34	0.1153	0.511814 (06)	0.511323	-9.3	1.96	2.02	Masberg et al. (2005)

Isotopic ratios with subscript 'i' were all age-corrected to an age of last metamorphic event.
T^{Nd}_{DM} = single and two-stage Nd model ages calculated after Liew and Hofmann (1988)
[a] In the parentheses are given analytical errors (2 s.e.) on the last two decimal places of the measured ratios.

the best time estimate for sedimentation of the upper part of the Neoproterozoic strata in the Central Kaoko Zone and in the Orogen Core unit provided by the age of youngest detrital zircons (this study) and the age of early metamorphism (Goscombe et al., 2003b; Jung et al., 2007). Transport of the detrital material from the Punta del Este – Coastal Terrane onto the attenuated Congo Craton margin suggests an active building of topography in the area westward of the Congo Craton margin and transport of sediments towards the east (in the present-day coordinates) (Fig. 9b). The exact timing of the sediment deposition in the upper part of the Neoproterozoic sedimentary cover is not known and the transport of detrital material from the west has two plausible explanations. The deposits may represent syn-orogenic (molasse-type) sediments from early stages of the Neoproterozoic collision that were later thrust under the upper plate of the Punta del Este – Coastal Terrane. An alternative explanation is in accord with the interpretation of Goscombe and Gray (2007, 2008) who suggested that at c. 650–630 Ma, when the Coastal Terrane of the Kaoko Belt was acting as a magmatic arc/back-arc domain, this unit was an integral part of the attenuated Congo Craton margin. The arc has been eroded after the cessation of magmatic activity, but prior to underthrusting of the Congo Craton margin below the magmatic arc domain (Fig. 9b). An unequivocal scenario cannot be determined based on data presented in this study. However, due to assumed large thickness of the post-650 Ma sediments (e.g. Guj, 1970) and their extensive pan-African metamorphism, we prefer the later model of pre-collisional sedimentation and subsequent involvement of these sediments into the collision of the Punta del Este – Coastal Terrane with the Congo Craton.

6. Conclusions

1) Metavolcanic rocks accompanying the bottom part of the Congo Craton metasedimentary cover in the Kaoko Belt yielded U–Pb zircon ages of c. 710, 730–735 and 740 Ma. The time span of the syn-rifting igneous activity is c. 30 Ma and its onset was temporally shifted by c. 15–25 Ma with respect to the same type of magmatism along the southern margin of the Congo Craton.
2) Dating of metamorphosed clastic sediments from the Central Kaoko Zone and Orogen Core units has shown the presence of two groups of samples with contrasting detrital zircon ages. Samples collected from the locations close to the Paleoproterozoic–Archean Congo Craton basement show dominance of Meso- and Paleoproterozoic zircons and some individual Archean grains, whereas samples collected higher up in the metasedimentary sequence are dominated by Neoproterozoic zircons and the proportion of Mesoproterozoic to Archean zircon grains is small. Detrital zircons from quartzites in the tectonically lowermost part of the Coastal Terrane also have mostly Meso- and Paleoproterozoic ages.
3) Comparison of the detrital zircon data with protolith zircon ages from potential source regions suggests the Congo/Kalahari Craton as a likely source of detritus for the bottom sequence of the Congo Craton cover. The clastic material from the upper parts of the Congo Craton cover has most probably originated in the Punta del Este – Coastal Terrane. This interpretation is compatible with contrasting Nd model ages for samples from the two inferred stratigraphic levels. The source of clastic material for the Coastal Terrane must have been similar to the crust of the Congo/Kalahari Craton.
4) The presence of c. 650 Ma detrital zircons in the upper part of the Neoproterozoic cover of the Congo Craton suggests proximity of the Punta del Este – Coastal Terrane and the Congo Craton margin already prior to the onset of their mutual collision. This finding supports the geodynamic model of Goscombe and Gray (2007, 2008) who suggested that the Coastal Terrane has developed as an arc/back-arc system along the attenuated margin of the Congo Craton at c. 650–630 Ma.

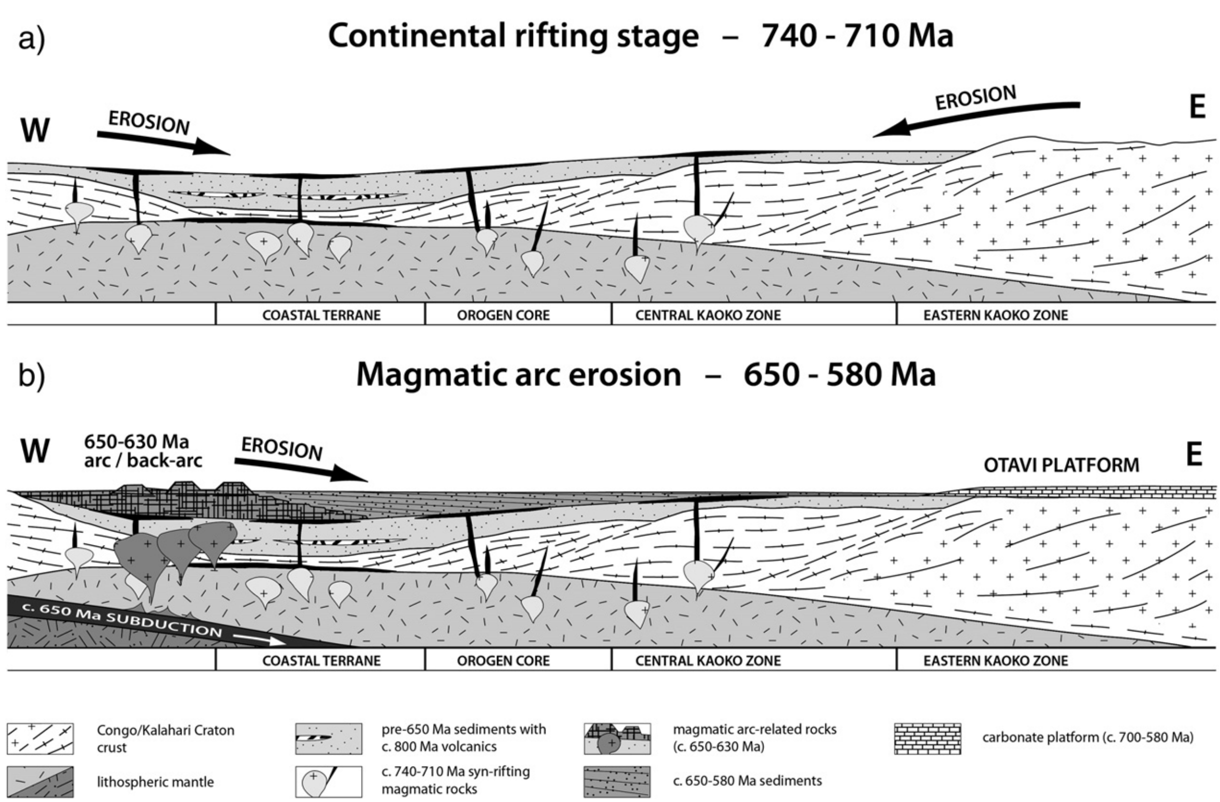

Fig. 9. Schematic (not to scale) cross-sections suggesting pre-collisional position of the principal tectonic units of the Kaoko Belt and sources of detrital material for its metasedimentary rocks. a) Erosion of the Congo Craton basement and sedimentation of the lowermost part of its cover during the continental rifting is accompanied by syn-rifting volcanism around 740–730 Ma. b) Erosion of c. 650–630 Ma volcanic arc and underlying older crust between c. 650 Ma (arc formation) and c. 570 Ma (onset of collision) provides clastic material for the upper part of the Congo Craton cover.

Acknowledgments

This project was supported by the Czech Science Foundation (Project No. P210/11/1904). The authors greatly appreciate numerous discussions with Charlie Hoffmann, the kind assistance of Ute Schreiber (both from the Geological Survey of Namibia), as well as the field assistance of Ouma Greyvensteyn and Andries Boerewors. We thank Martin Whitehouse and Lev Ilyinsky for their support while using the Nordsim ion probe in Stockholm. The Nordsim facility is jointly funded by Denmark, Finland, Norway, Sweden and Iceland (this is Nordsim publication # 345). We are grateful to the staff of the Radiogenic Isotopes Laboratory (Czech Geological Survey, Prague) for providing Nd isotopic data. Comments of two anonymous reviewers helped to improve the manuscript.

Appendix A. Analytical techniques

A.1. Zircon separation techniques

Approximately 1 to 2 kg of rock material for each sample was crushed and disintegrated using disk mill to obtain grain fraction between c. 50–500 μm in size. The samples were loaded to sodium polytungstate (SPT) and subsequently to diiodomethane (DIM) heavy liquids, followed by the removal of the magnetic minerals from the heavy fraction using the Frantz isodynamic separator. Zircons were then transferred in ethanol from the pool of separated grains to a double-sided tape using pipette and mounted in 1 inch epoxy-filled blocks and polished using SiC and diamond paste to obtain even surfaces suitable for cathodoluminescence imaging and laser ablation ICP-MS analysis.

A.2. Zircon imaging and LA-ICP-MS techniques

Cathodoluminescence images of zircons were obtained using a Zeiss Supra 55 VP scanning electron microscope at the University of Bergen. Prior to analysis, the carbon coating was removed and the sample surfaces were cleaned with 2% HNO_3, DI water, and ethanol. Isotopic analysis of zircons by laser ablation ICP-MS followed the technique described in Košler et al. (2002). A Thermo-Finnigan Element 2 sector field ICP-MS coupled to a 193 ArF Excimer laser (Resonetics RESOlution M50-LR) at Bergen University was used to measure Pb/U and Pb isotopic ratios in zircons. The sample introduction system was modified to enable simultaneous nebulization of a tracer solution and laser ablation of the solid sample (Horn et al., 2000). Natural Tl ($^{205}Tl/^{203}Tl = 2.3871$ — Dunstan et al., 1980), ^{209}Bi and enriched ^{233}U and ^{237}Np (>99%) were used in the tracer solution, which was aspirated to the plasma in an argon–helium carrier gas mixture through an Apex desolvation nebulizer (Elemental Scientific) and a T-piece tube attached to the back end of the plasma torch. A helium gas line carrying the sample from the laser cell to the plasma was also attached to the T-piece tube. The laser was set up to produce energy density of ca 7 J/cm^2 at a repetition rate of 5 Hz. The laser beam was imaged on the surface of the sample placed in the two-volume ablation cell, which was mounted on a computer-driven motorized stage of a microscope. During ablation the stage was moved beneath the stationary laser beam (19–26 μm in diameter) to produce a linear raster in the sample. Typical acquisitions consisted of a 35 second measurement of analytes in the gas blank and aspirated solution, particularly ^{203}Tl–^{205}Tl–^{209}Bi–^{233}U–^{237}Np, followed by the measurement of U and Pb signals from zircon, along with the continuous signal from the aspirated solution, for another 120 s. The data were acquired in a time resolved – peak jumping – pulse counting mode with 1 point measured per peak for masses 202 (flyback), 203 and 205 (Tl), 206 and 207 (Pb), 209 (Bi), 233 (U), 237 (Np), 238 (U), 249 (233U oxide), 253 (237 Np oxide) and 254 (238U oxide). Raw data were corrected for dead time of the electron multiplier and processed off line in a spreadsheet-based program Lamdate (Košler et al., 2002) and plotted on concordia diagrams using Isoplot (Ludwig, 1999). Data reduction included correction for gas blank, laser-induced elemental fractionation of Pb and U and instrument mass bias. Minor formation of oxides of U and Np was corrected for by adding signal intensities at masses 249, 253 and 254 to the intensities at masses 233, 237 and 238, respectively. No common Pb correction was applied to the data. Details of data reduction and corrections are described in Košler et al. (2002) and Košler and Sylvester (2003). Zircon reference material 91500 (1065 Ma — Wiedenbeck et al., 1995), GJ-1 (609 Ma — Jackson et al., 2004) and Plešovice (337 Ma — Sláma et al., 2008) were periodically analyzed during this study and they yielded pooled concordia ages of 1086 ± 9, 600 ± 4 and 342 ± 2 Ma, respectively.

A.3. SIMS technique

Prior to the SIMS analysis, the samples were coated with c. 30 nm of gold and analyzed for isotopes of U, Pb and interfering molecules on a Cameca IMS 1280 ion probe at the Swedish.

Museum of Natural History in Stockholm (Nordsim facility). The instrument parameters, analytical method, calibration and correction procedures were similar to those described by Whitehouse et al. (1999) and Whitehouse and Kamber (2005). The instrument was operated in automated mode with 18 μm ion beam diameter. The measured Pb/U ratios were calibrated against the reference zircon 91500, which has an age of 1065.4 ± 0.3 Ma and U and Pb concentrations of 80 and 15 ppm, respectively (Wiedenbeck et al., 1995). Common lead corrections assumed a modern-day average terrestrial common Pb composition (Stacey and Kramers, 1975).

A.4. Sm–Nd isotopic compositions

For the radiogenic isotope determinations, samples were dissolved using a combined HF–HCl–HNO_3 acid attack. The bulk REE were isolated by exchange chromatography techniques following the procedure of Pin et al. (1994) (PP columns filled with TRU.spec Eichrom resin). The Nd was further separated from the REE fraction on PP columns with Ln.spec Eichrom resin (Pin and Zalduegui, 1997). Complete analytical details were reported by Míková and Denková (2007).

Isotopic analyses were performed on a Finnigan MAT 262 thermal ionization mass spectrometer housed at the Czech Geological Survey in dynamic mode using a single Re filament with Ta addition for Sr measurement and double Re filament assembly for Nd. The $^{143}Nd/^{144}Nd$ ratios were corrected for mass fractionation to $^{146}Nd/^{144}Nd = 0.7219$ (Wasserburg et al., 1981). External reproducibility was estimated from repeat analyses of the BCR-1 ($^{143}Nd/^{144}Nd = 0.512621 \pm 20$ (2σ, n = 5)) isotopic standard. The Sm and Nd concentrations were obtained by ICP-MS.

The decay constants applied to age-correct the isotopic ratios are from Lugmair and Marti (1978). The ε_{Nd} values were obtained using Bulk Earth parameters of Jacobsen and Wasserburg (1980), the two-stage Depleted Mantle Nd model ages (T^{Nd}_{DM}) were calculated after Liew and Hofmann (1988).

Appendix B. Supplementary data

Supplementary data to this article can be found online at http://dx.doi.org/10.1016/j.gr.2013.06.021.

References

Babinski, M., Chemale Jr., F., van Schmus, W.R., Hartmann, L.A., da Silva, L.C., 1997. U–Pb and Sm–Nd geochronology of the Neoproterozoic granitic–gneissic Dom Feliciano Belt, southern Brazil. Journal of South American Earth Sciences 10, 263–274.

Basei, M.A.S., Frimmel, H.E., Nutman, A.P., Preciozzi, F., Jacob, J., 2005. A connection between the Neoproterozoic Dom Feliciano (Brazil/Uruguay) and Gariep (Namibia/South Africa) orogenic belts — evidence from a reconnaissance provenance study. Precambrian Research 139, 195–221.

Basei, M.A.S., Frimmel, H.E., Nutman, A.P., Preciozzi, F., 2008. West Gondwana amalgamation based on detrital zircon ages from Neoproterozoic Ribeira and Dom Feliciano belts of South America and comparison with coeval sequences from SW Africa. In: Pankhurst, R.J., Trouw, R.A.J., Brito Neves, B.B., de Wit, M.J. (Eds.), West Gondwana: Pre-Cenozoic Correlations Across the South Atlantic Region. Geological Society, London, Special Publications, 294, pp. 239–256.

Basei, M.A.S., Peel, E., Sánchez Bettucci, L., Preciozzi, F., Nutman, A.P., 2011. The basement of the Punta del Este Terrane (Uruguay): an African Mesoproterozoic fragment at the eastern border of the South American Río de La Plata craton. International Journal of Earth Sciences 100, 289–304.

Becker, T., Schreiber, U., Kampunzu, A.B., Armstrong, R., 2006. Mesoproterozoic rocks of Namibia and their plate tectonic setting. Journal of African Earth Sciences 46, 112–140.

Bjerkgard, T., Stein, H.J., Bingen, B., Henderson, I.H.C., Sanstad, J.S., Moinz, A., 2009. The Niassa Gold Belt, northern Mosambique — a segment of a continental-scale Pan-African gold-bearing structure? Journal of African Earth Sciences 53, 45–58.

Borg, G., Kärner, K., Buxton, M., Armstrong, R., Van der Merwe, S.W., 2003. Geology of the Skorpion zinc deposit, southern Namibia. Economic Geology 98, 749–771.

Chemale Jr., F., Mallmann, G., Bitencourt, M.F., Kawashita, K., 2012. Time constraints on magmatism along the Major Gercino Shear Zone, southern Brazil: Implications for West Gondwana reconstruction. Gondwana Research 22, 184–199.

da Silva, L.C., Hartmann, L.A., McNaughton, N.J., Fletcher, I.R., 1999. SHRIMP U/Pb zircon dating of Neoproterozoic granitic magmatism and collision in the Pelotas Batolith, southernmost Brazil. International Geology Review 41, 531–551.

Dingeldey, D.P., Dürr, S.B., Charlesworth, E.G., Franz, L., Okrusch, M., Stanistreet, I.G., 1994. A geotraverse through the northern coastal branch of the Damaran orogen west of Sesfontein, Namibia. Journal of African Earth Sciences 19, 315–329.

Dunstan, L.P., Gramch, J.W., Barnes, I.L., Purdy, W.C., 1980. The absolute abundance and the atomic weight of a reference sample of thallium. Journal of Research of the National Bureau of Standards 85, 1–10.

Franz, L., Romer, R.L., Dingeldey, D.P., 1999. Diachronous Pan-African granulite-facies metamorphism (650 Ma and 550 Ma) in the Kaoko Belt, NW Namibia. European Journal of Mineralogy 11, 167–180.

Frimmel, H.E., Klötzli, U., Siegfried, P., 1996. New Pb–Pb single zircon age constraints on the timing of Neoproterozoic glaciation and continental break-up in Namibia. Journal of Geology 104, 459–469.

Frimmel, H.E., Zartman, R.E., Späth, A., 2001. The Richtersveld Igneous Complex, South Africa: U–Pb zircon and geochemical evidence for the beginning of Neoproterozoic continental breakup. Journal of Geology 109, 493–508.

Frimmel, H.E., Basei, M.S., Gaucher, C., 2011. Neoproterozoic geodynamic evolution of SW-Gondwana: a southern African perspective. International Journal of Earth Sciences 100, 323–354.

Goldstein, S.L., O'Nions, R.K., Hamilton, P.J., 1984. A Sm–Nd isotopic study of atmospheric dusts and particulates from major river systems. Earth and Planetary Science Letters 70, 221–236.

Goscombe, B.D., 1998a. Geological map of Tomakas 1:50,000 sheet. Geological Survey of Namibia.

Goscombe, B.D., 1998b. Geological map of Omapungwe 1:50,000 sheet. Geological Survey of Namibia.

Goscombe, B., Gray, D.R., 2007. The Coastal Terrane of the Kaoko Belt, Namibia: outboard arc-terrane and tectonic significance. Precambrian Research 155, 139–158.

Goscombe, B., Gray, D.R., 2008. Structure and strain variation at mid-crustal levels in a transpressional orogen: a review of Kaoko Belt structure and the character of West Gondwana amalgamation and dispersal. Gondwana Research 13, 45–85.

Goscombe, B., Hand, M., Gray, D., 2003a. Structure of the Kaoko Belt, Namibia: progressive evolution of a classic transpressional orogen. Journal of Structural Geology 25, 1049–1081.

Goscombe, B., Hand, M., Mawby, J., Gray, D., 2003b. The metamorphic architecture of a transpressional orogen: the Kaoko Belt, Namibia. Journal of Petrology 44, 679–711.

Goscombe, B., Gray, D., Armstrong, R., Foster, D.A., Vogl, J., 2005. Event geochronology of the Pan-African Kaoko Belt, Namibia. Precambrian Research 140, 103.e1–103.e41.

Gross, A.O.M.S., Droop, G.T.R., Porcher, C.C., Fernandes, L.A.D., 2009. Petrology and thermobarometry of mafic granulites and migmatites from the Chafalote Metamorphic Suite: new insights into the Neoproterozoic *P–T* evolution of the Uruguayan—Sul-Rio-Grandense shield. Precambrian Research 170, 157–174.

Guj, P., 1970. The Damara mobile belt in the south-western Kaokoveld, South West Africa. University of Cape Town Precambrian Research Unit Bulletin, 10 (168 pp.).

Halverson, G.P., Hoffman, P.F., Schrag, D.P., Maloof, A.C., Rice, A.H.N., 2005. Toward a Neoproterozoic composite carbon-isotope record. Geological Society of America Bulletin 117, 1181–1207.

Hartmann, L.A., Santos, J.O., Bossi, J., Campal, N., Schipilov, A., McNaughton, N., 2002. Zircon and titanite U–Pb SHRIMP geochronology of Neoproterozoic felsic magmatism on the eastern border of the Río de la Plata Craton, Uruguay. Journal of South American Earth Sciences 15, 229–236.

Hedberg, R.M., 1979. Stratigraphy of the Owamboland basin, South West Africa. University of Cape Town Precambrian Research Unit Bulletin, 24 (325 pp.).

Hoffman, P.F., Hawkins, D.P., Isachen, C.E., Bowring, S.A., 1996. Precise U–Pb zircon ages for early Damaran magmatism in the Summas Mountains and Welwitschia Inlier, northern Damara belt, Namibia. Communications of the Geological Survey of Namibia 11, 47–52.

Hoffmann, K.-H., Prave, A.R., 1996. A preliminary note on a revised subdivision and regional correlation of the Otavi Group based on glaciogenic diamictites and associated cap dolostones. Communications of the Geological Survey of Namibia 11, 77–82.

Hoffmann, K.-H., Condon, D.J., Bowring, S.A., Crowley, J.L., 2004. U–Pb zircon date from the Neoproterozoic Ghaub Formation, Namibia: constraints on Marinoan glaciation. Geology 32, 817–820.

Horn, I., Rudnick, R.L., McDonough, W.F., 2000. Precise elemental and isotope ratio measurement by simultaneous solution nebulisation and laser ablation-ICP-MS: application to U–Pb geochronology. Chemical Geology 164, 281–301.

Jackson, S.E., Pearson, N., Griffin, W.L., Belousova, E.A., 2004. The application of laser ablation-inductively coupled plasma-mass spectrometry to in situ U–Pb zircon geochronology. Chemical Geology 211, 47–69.

Jacobsen, S.B., Wasserburg, G.J., 1980. Sm–Nd isotopic evolution of chondrites. Earth and Planetary Science Letters 50, 139–155.

Janoušek, V., Farrow, C.M., Erban, V., 2006. Interpretation of whole-rock geochemical data in igneous geochemistry: introducing Geochemical Data Toolkit (GCDkit). Journal of Petrology 47, 1255–1259.

Janoušek, V., Konopásek, J., Ulrich, S., Erban, V., Tajčmanová, L., Jeřábek, P., 2010. Geochemical character and petrogenesis of Pan-African Amspoort suite of the Boundary Igneous Complex in the Kaoko Belt (NW Namibia). Gondwana Research 18, 688–707.

Jung, S., Kröner, A., Kröner, S., 2007. A 700 Ma Sm–Nd garnet–whole rock age from the granulite facies Central Kaoko Zone (Namibia): evidence for a cryptic high-grade polymetamorphic history? Lithos 97, 247–270.

Key, R.M., Liyungu, A.K., Njamu, F.M., Somwe, V., Banda, J., Mosley, P.N., Armstrong, R.A., 2001. The western arm of the Lufilian Arc in NW Zambia and its potential for copper mineralization. Journal of African Earth Sciences 33, 503–528.

Konopásek, J., Kröner, S., Kitt, S.L., Passchier, C.W., Kröner, A., 2005. Oblique collision and evolution of large-scale transcurrent shear zones in the Kaoko belt, NW Namibia. Precambrian Research 136, 139–157.

Konopásek, J., Košler, J., Tajčmanová, L., Ulrich, S., Kitt, S.L., 2008. Neoproterozoic igneous complex emplaced along major tectonic boundary in the Kaoko Belt (NW Namibia): ion probe and LA-ICP-MS dating of magmatic and metamorphic zircons. Journal of the Geological Society of London 165, 153–165.

Košler, J., Sylvester, P., 2003. Present trends and the future of zircon in geochronology: laser ablation ICPMS. In: Hanchar, J.M., Hoskin, P.W.O. (Eds.), Zircon. Reviews in Mineralogy and Geochemistry, 53, pp. 243–275.

Košler, J., Fonneland, H., Sylvester, P., Tubrett, M., Pedersen, R.B., 2002. U–Pb dating of detrital zircons for sediment provenance studies — a comparison of laser ablation ICPMS and SIMS techniques. Chemical Geology 182, 605–618.

Kröner, S., Konopásek, J., Kröner, A., Passchier, C.W., Poller, U., Wingate, M.T.D., Hofmann, K.H., 2004. U–Pb and Pb–Pb zircon ages for metamorphic rocks in the Kaoko Belt of northwestern Namibia: a Palaeo- to Mesoproterozoic basement reworked during the Pan-African orogeny. South African Journal of Geology 107, 455–476.

Kröner, A., Rojas–Agramonte, Y., Hegner, E., Hoffmann, K.-H., Wingate, M.T.D., 2010. SHRIMP zircon dating and Nd isotopic systematics of Palaeoproterozoic migmatitic orthogneisses in the Epupa Metamorphic Complex of northwestern Namibia. Precambrian Research 183, 50–69.

Lenz, C., Fernandes, L.A.D., McNaughton, N.J., Porcher, C.C., Masquelin, H., 2011. U–Pb SHRIMP ages for the Cerro Bori Orthogneisses, Dom Feliciano Belt in Uruguay: evidences of a 800 Ma magmatic and 650 Ma metamorphic event. Precambrian Research 185, 149–163.

Liew, T.C., Hofmann, A.W., 1988. Precambrian crustal components, plutonic associations, plate environment of the Hercynian Fold Belt of Central Europe: indications from a Nd and Sr isotopic study. Contributions to Mineralogy and Petrology 98, 129–138.

Ludwig, K.R., 1999. IsoplotEx v. 2.6. Berkeley Geochronological Center Special Publication, no. 1a.

Luft Jr., J.L., Chemale Jr., F., Armstrong, R., 2011. Evidence of 1.7- to 1.8-Ga collisional arc in the Kaoko Belt, NW Namibia. International Journal of Earth Sciences 100, 305–321.

Lugmair, G.W., Marti, K., 1978. Lunar initial $^{143}Nd/^{144}Nd$: differential evolution line of the lunar crust and mantle. Earth and Planetary Science Letters 39, 349–357.

Martin, H., 1965. The Precambrian geology of South West Africa and Namaqualand. University of Cape Town Precambrian Research Unit Bulletin, 4 (159 pp.).

Masberg, P., Mihm, D., Jung, S., 2005. Major and trace element and isotopic (Sr, Nd, O) constraints for Pan-African crustally contaminated grey granite gneisses from the southern Kaoko Belt, Namibia. Lithos 84, 25–50.

Masquelin, H., Fernandes, L.A.D., Lenz, C., Porcher, C.C., McNaughton, N.J., 2012. The Cerro Olivo Complex: a pre-collisional Neoproterozoic magmatic arc in Eastern Uruguay. International Geology Review 54, 1161–1183.

Míková, J., Denková, P., 2007. Modified chromatographic separation scheme for Sr and Nd isotope analysis in geological silicate samples. Journal of Geosciences 52, 221–226.

Miller, R.M., 1983. The Pan-African Damara Orogen of South West Africa/Namibia. In: Miller, R.M. (Ed.), Evolution of the Damara Orogen of South West Africa/Namibia. Geological Society of South Africa Special Publications, 11, pp. 431–515.

Oyhantçabal, P., Siegesmund, S., Wemmer, K., Presnyakov, S., Layer, P., 2009. Geochronological constraints on the evolution of the southern Dom Feliciano Belt (Uruguay). Journal of the Geological Society of London 166, 1075–1084.

Pin, C., Zalduegui, J.F.S., 1997. Sequential separation of light rare-earth elements, thorium and uranium by miniaturized extraction chromatography: application to isotopic analyses of silicate rocks. Analytica Chimica Acta 339, 79–89.

Pin, C., Briot, D., Bassin, C., Poitrasson, F., 1994. Concomitant separation of strontium and samarium–neodymium for isotopic analysis in silicate samples, based on specific extraction chromatography. Analytica Chimica Acta 298, 209–217.

Porada, H., 1989. Pan-African rifting and orogenesis in southern to equatorial Africa and eastern Brazil. Precambrian Research 44, 103–136.

Prave, A.R., 1996. Tale of three cratons: Tectonostratigraphic anatomy of the Damara orogen in northwestern Namibia and the assembly of Gondwana. Geology 24, 1115–1118.

Seth, B., Kröner, A., Mezger, K., Nemchin, A.A., Pidgeon, R.T., Okrusch, M., 1998. Archaean to Neoproterozoic magmatic events in the Kaoko Belt of NW Namibia and their geodynamic significance. Precambrian Research 92, 341–363.

Seth, B., Jung, S., Hoernes, S., 2002. Isotope constraints on the origin of Pan-African granitoid rocks in the Kaoko Belt, NW Namibia. South African Journal of Geology 105, 179–192.

Seth, B., Armstrong, R.A., Brandt, S., Villa, I.M., Kramers, J.D., 2003. Mesoproterozoic U–Pb and Pb–Pb ages of granulites in NW Namibia: reconstructing a complete orogenic cycle. Precambrian Research 126, 147–168.

Seth, B., Jung, S., Gruner, B., 2008. Deciphering polymetamorphic episodes in high-grade metamorphic orogens: constraints from PbSL, Sm/Nd and Lu/Hf garnet dating of low- to high-grade metasedimentary rocks from the Kaoko Belt (Namibia). Lithos 104, 131–146.
Singletary, S.J., Hanson, R.E., Martin, M.W., Crowley, J.L., Bowring, S.A., Key, R.M., Ramokate, L.V., Direng, B.B., Krol, M.A., 2003. Geochronology of basement rocks in the Kalahari Desert, Botswana, and implications for regional Proterozoic tectonics. Precambrian Research 121, 47–71.
Sláma, J., Košler, J., Condon, D.J., Crowley, J.L., Gerdes, A., Hanchar, J.M., Horstwood, M., Morris, G.A., Nasdala, L., Norbert, N., Schaltegger, U., Schoene, B., Tubrett, M.N., Whitehouse, M.J., 2008. Plešovice zircon — a new natural reference material for U–Pb and Hf isotopic microanalysis. Chemical Geology 249, 1–35.
Stacey, J.S., Kramers, J.D., 1975. Approximation of terrestrial lead isotope evolution by a two-stage model. Earth and Planetary Science Letters 26, 207–221.
Ulrich, S., Konopásek, J., Jeřábek, P., Tajčmanová, L., 2011. Transposition of structures in the Neoproterozoic Kaoko Belt (NW Namibia) and their absolute timing. International Journal of Earth Sciences 100, 415–429.
Vermeesch, P., 2012. On the visualisation of detrital age distributions. Chemical Geology 312, 190–194.
Wasserburg, G.J., Jacobsen, S.B., DePaolo, D.J., McCulloch, M.T., Wen, T., 1981. Precise determination of Sm/Nd ratios, Sm and Nd isotopic abundances in standard solutions. Geochimica et Cosmochimica Acta 45, 2311–2324.
Whitehouse, M.J., Kamber, B.S., 2005. Assigning dates to thin gneissic veins in high-grade metamorphic terranes: a cautionary tale from Akilia, southwest Greenland. Journal of Petrology 46, 291–318.
Whitehouse, M.J., Kamber, B.S., Moorbath, S., 1999. Age significance of U–Th–Pb zircon data from early Archaean rocks of west Greenland—a reassessment based on combined ion-microprobe and imaging studies. Chemical Geology 160, 201–224.
Wiedenbeck, M., Alle, P., Corfu, F., Griffin, W.L., Meier, M., Oberli, F., von Quadt, A., Roddick, J.C., Spiegel, W., 1995. Three natural zircon standards for U–Th–Pb, Lu–Hf, trace element and REE analyses. Geostandards Newsletter 19, 1–23.
Will, T.M., Okrusch, M., Gruner, B.B., 2004. Barrovian and Buchan type metamorphism in the Pan-African Kaoko Belt, Namibia: implications for its geotectonic position within the framework of Western Gondwana. South African Journal of Geology 107, 431–454.